

The Luminosities and Distance Scales of Type II Cepheid and RR Lyrae variables

Michael W. Feast¹, Clifton D. Laney², Thomas D. Kinman³, Floor van Leeuwen⁴,
 Patricia A. Whitelock^{1,2,5}

¹ *Astronomy Department, University of Cape Town, 7701, Rondebosch, South Africa.*
 (email: mwf@artemisia.ast.uct.ac.za)

² *South African Astronomical Observatory, P.O. Box 9, 7935, Observatory, South Africa.*

³ *National Optical Astronomy Observatory, Tucson, P.O. Box 26732, AZ85726, USA.*

⁴ *Institute of Astronomy, Madingley Rd., Cambridge, England.*

⁵ *National Astrophysics and Space Science Programme, Department of Mathematics and Applied Mathematics, University of Cape Town, 7701, South Africa.*

30 October 2018

ABSTRACT

Infrared and optical absolute magnitudes are derived for the type II Cepheids κ Pav and VY Pyx using revised Hipparcos parallaxes and for κ Pav, V553 Cen and SW Tau from pulsation parallaxes. Revised Hipparcos and HST (Benedict et al.) parallaxes for RR Lyrae agree satisfactorily and are combined in deriving absolute magnitudes. Phase-corrected J, H, K_s mags are given for 142 Hipparcos RR Lyraes based on 2MASS observations. Pulsation and trigonometrical parallaxes for classical Cepheids are compared to establish the best value for the projection factor (p) used in pulsational analyses.

The M_V of RR Lyrae itself is 0.16 ± 0.12 mag brighter than predicted from a $M_V - [Fe/H]$ relation based RR Lyrae stars in the LMC at a modulus of 18.39 ± 0.05 as found from classical Cepheids. This is consistent with the prediction of Catalan & Cortés that it is over luminous for its metallicity. The M_{K_s} results for the metal- and carbon-rich, Galactic disc stars, V553 Cen and SW Tau, each with small internal errors (± 0.08 mag) have a mean deviation of only 0.02 mag from the Period-Luminosity relation established by Matsunaga et al. for type II Cepheids in globular clusters and with a zero-point based on the same LMC scale. Comparing directly the luminosities of these two stars with published data on Type II Cepheids in the LMC and in the Galactic Bulge leads to an LMC modulus of 18.37 ± 0.09 and a distance to the Galactic Centre of $R_0 = 7.64 \pm 0.21$ kpc. The data for VY Pyx agree with these results within the uncertainties set by its parallax. Evidence is presented that κ Pav may have a close companion and possible implications of this are discussed. If the pulsation parallax of this star is incorporated in the analyses the distance scales just discussed will be increased by $\sim 0.15 \pm 0.15$ mag. V553 Cen and SW Tau show that at optical wavelengths PL relations are wider for field stars than for those in globular clusters. This is probably due to a narrower range of masses in the latter case.

Key words:

1 INTRODUCTION

The RR Lyrae variables are known, primarily from studies of globular clusters, to lie on or immediately above the Horizontal branch (HB) in an HR diagram. Globular cluster studies also show a class of variable stars lying in an instability strip in an HR diagram which extends approximately 3 mag above the HB. Variables with similar characteristics are also found in the general field, both in the halo and disc.

All these variables, both in clusters and the field are classed together as “type II Cepheids” (CephIIs). These stars have been divided into three classes according to their periods. Those of short period (roughly $P < 7$ days) are called BL Her stars, whilst longer period ones (up to $P \sim 20$ days) are called W Vir stars. At even longer periods, many of the CephIIs show characteristic alternations of deep and shallow minima and are classed as RV Tau stars. This subdivision of

CephIIs has not been universally adopted. Thus Sandage & Tammann (2006) review and summarize a system of classification based on light-curve parameters that relate to their population characteristic and these partially correlate with their metallicities. It should be noted that the “population II Cepheids” with which Sandage & Tammann are primarily concerned are a subset of the “type II Cepheids”. Maas et al. (2007) have shown that the shorter period CephIIs in the general field differ from those of longer period in their detailed chemical composition. The short period stars are generally believed (Gingold 1976, 1985) to be evolving across the instability strip from the HB towards the AGB. The longer period stars, on the other hand, are believed to be on blueward excursions into the instability strip from the AGB due to shell flashing.

In the present paper we discuss the luminosities of RR Lyrae and CephIIs on the basis of the revised Hipparcos trigonometrical parallaxes (van Leeuwen 2007a, see also van Leeuwen 2007b) and newly derived pulsation parallaxes for three CephII variables.

2 PERIOD-LUMINOSITY AND METALLICITY-LUMINOSITY RELATIONS

Here we present various relations which are required in the interpretation of our data.

2.1 Relationships for RR Lyrae variables

It has long been thought that the luminosities of RR Lyrae variables can be expressed in the form:

$$M_V = a[Fe/H] + b \quad (1)$$

However, the values of a and b have been much disputed, as has the question of the linearity of the equation. In the following we adopt:

$$M_V = 0.214[Fe/H] + (19.39 - Mod(LMC)). \quad (2)$$

This is based on RR Lyraes in the LMC (Gratton et al. 2004). Adopting an LMC modulus of 18.39^1 as derived from classical Cepheids (Benedict et al. 2007, van Leeuwen et al. 2007), the constant term becomes:

$$b = +1.0.$$

The LMC RR Lyraes, on which this relation is based, cover a range in $[Fe/H]$ from ~ -0.8 to -2.2 , but are mainly concentrated between -1.3 and -1.8 . There is evidence, however, that the slope of the relation is not universal. Clementini et al. (2005) find that in the Sculptor dwarf spheroidal, over roughly the same metallicity range, the slope is 0.092 ± 0.027 compared with the LMC 0.214 ± 0.047 and they suggest that the Sculptor RR Lyraes are on average more evolved than those in the LMC.

That there is a period-luminosity relation for RR Lyraes in the K band ($PL(K)$), possibly independent, or nearly independent of metallicity, goes back at least to the work of

Longmore et al. (1986) on globular clusters. The most recent version of such a relation was given by Sollima et al. (2006) again based on globular clusters. The relative distances of the clusters came from main-sequence fitting and the zero-point of their final relation was set by a trigonometrical parallax of RR Lyrae itself (Benedict et al. 2002). They found:

$$M_{K_s} = -2.38(\pm 0.04) \log P + 0.08(\pm 0.11)[Fe/H] - 1.05(\pm 0.13), \quad (3)$$

where K_s is the K_s magnitude in the 2MASS system. The term in $[Fe/H]$ is small and not statistically significant.

2.2 Relationships for type II Cepheids

In the past various PL relations for CephIIs at visual wavelengths have been suggested based primarily on globular cluster work. More recently, it was shown from globular cluster data that a well defined $PL(K_s)$ relation, with small scatter, applied (Matsunaga et al. 2006). The globular cluster distances were determined from a relation for horizontal branch stars similar to eq. 2 and we may write the Matsunaga CephII relation as:

$$M_{K_s} = -2.41(\pm 0.05) \log P + c, \quad (4)$$

where $c = 17.39 - Mod(LMC)$

and $c = -1.0$ for $Mod(LMC) = 18.39$ as above.

The (internal) standard error of the constant term is ± 0.02 at the mean $\log P$ (1.120). Matsunaga et al. pointed out that RR Lyraes in clusters lay on an extrapolation of this relation to shorter periods. The subsequent work of Sollima et al. (2006) confirms this (compare eqs. 3 and 4). Matsunaga et al. examined their data for a metallicity effect on the $PL(K)$ zero-point and found a term, -0.10 ± 0.06 . This is clearly not significant and is of opposite sign to the metallicity term in the RR Lyrae relation (eq. 3) which is also not significant. This suggests that a combined RR Lyrae/CephII $PL(K)$ is virtually metal independent in globular clusters. Some caution is necessary in accepting this, however, since there are only four CephIIs in the Matsunaga sample with $[Fe/H] > -1.0$ and these all have periods greater than 10 days².

In addition to the above the following three PL relations at optical wavelengths will be required later. They are based on CephIIs in NGC 6441 and 6388 and are taken directly from Pritzl et al. (2003).

$$M_V = -1.64(\pm 0.05) \log P + 0.05(\pm 0.05), \quad (5)$$

$$M_B = -1.23(\pm 0.09) \log P + 0.31(\pm 0.09), \quad (6)$$

$$M_I = -2.03(\pm 0.03) \log P - 0.36(\pm 0.01). \quad (7)$$

3 THE RR LYRAE VARIABLES

3.1 Data

Table 1 lists the data for 142 RR Lyrae variables.

¹ This includes a correction for metallicity effects based on Marci et al. 2006.

² But see the discussion of the field variables below.

Table 1: Basic data used in the analysis.

Hipparcos	name	π (mas)	$\Delta\pi$	V	J (mag)	H	K_s	P (day)	[Fe/H]	$E_{(B-V)}$ (mag)	typ
226	RU Scl	0.99	1.96	10.220	9.474	9.294	9.229	0.493347	-1.27	0.018	
320	UU Cet	1.59	5.73	12.080	11.137	10.863	10.837	0.606080	-1.28	0.021	
1878	SW And	-0.01	1.84	9.710	8.809	8.578	8.505	0.442262	-0.24	0.038	
2655	RX Cet	3.24	4.74	11.440	10.606	10.378	10.319	0.573685	-1.28	0.025	
4541	W Tuc	5.37	2.41	11.410	10.594	10.373	10.344	0.642260	-1.57	0.021	
4725	RU Cet	7.14	4.62	11.680	10.597	10.487	10.465	0.586267	-1.66	0.023	
5803	RU Psc	1.30	2.08	10.190	9.347	9.162	9.117	0.390333	-1.75	0.043	c
6029	XX And	-0.79	2.50	10.680	9.727	9.488	9.409	0.722755	-1.94	0.039	
6094	VW Scl	2.34	2.79	11.030	10.418	10.193	10.136	0.510913	-0.84	0.016	
6115	AM Tuc	-1.93	2.28	11.670	10.865	10.617	10.563	0.405769	-1.49	0.023	c
7149	RR Cet	0.48	1.85	9.730	8.829	8.623	8.520	0.553030	-1.45	0.022	
7398	VX Scl	3.71	3.64	12.020	11.094	10.894	10.853	0.637058	-2.25	0.014	
8163	SV Scl	5.50	2.37	11.380	10.718	10.596	10.543	0.377380	-1.77	0.014	c
8939	CI And	0.77	5.87	12.280	11.182	11.018	11.185	0.484728	-0.69	0.062	
9932	SS For	3.57	1.98	10.190	9.546	9.305	9.246	0.495424	-0.94	0.014	
10491	RV Cet	2.16	2.70	10.920	9.903	9.580	9.520	0.623350	-1.60	0.024	
11517	RZ Cet	-0.04	4.92	11.850	11.031	10.787	10.737	0.510606	-1.36	0.029	
12199	CS Eri	2.70	1.10	9.000	8.144	8.014	7.973	0.311332	-1.41	0.018	c
14601	X Ari	0.99	1.90	9.570	8.365	8.042	7.941	0.651154	-2.43	0.180	
14856	SV Eri	3.18	2.53	9.960	8.958	8.710	8.642	0.713865	-1.70	0.085	
16321	SX For	-5.39	2.38	11.120	10.035	9.847	9.772	0.605342	-1.66	0.012	
19993	AR Per	-1.32	2.02	10.510	9.012	8.710	8.642	0.425551	-0.30	0.108	
22442	RX Eri	1.31	1.70	9.690	8.737	8.485	8.429	0.587246	-1.33	0.058	
22466	U Pic	3.21	2.21	11.380	10.689	10.464	10.381	0.440373	-0.72	0.009	
22750	BB Eri	5.44	3.58	11.520	10.321	10.147	10.110	0.569909	-1.32	0.048	
22952	U Lep	2.32	2.97	10.570	9.814	9.565	9.542	0.581479	-1.78	0.027	
24471	RY Col	3.35	1.79	10.900	10.254	9.732	9.699	0.478832	-0.91	0.026	
29528	RX Col	-4.02	5.53	12.720	11.634	11.393	11.313	0.593780	-1.70	0.082	
34743	TZ Aur	-3.70	6.39	11.910	10.975	10.771	10.731	0.391676	-0.79	0.037	
35281	AA CMi	1.40	5.22	11.570	10.570	10.384	10.281	0.476327	-0.15	0.011	
35584	HH Pup	2.39	2.53	11.290	10.248	10.044	9.975	0.390748	-0.50	0.158	
35667	RR Gem	0.43	3.24	11.380	10.566	10.306	10.275	0.397292	-0.29	0.054	
37779	HK Pup	-2.90	3.60	11.370	10.240	10.010	9.915	0.734229	-1.11	0.160	
37805	TW Lyn	-6.62	8.60	12.000	11.075	10.854	10.778	0.481862	-0.66	0.051	
38561	SZ Gem	6.04	4.19	11.750	11.072	10.798	10.748	0.501143	-1.46	0.013	
39009	UY Cam	0.19	1.99	11.530	11.002	10.872	10.859	0.267044	-1.33	0.022	c
39849	XX Pup	-0.15	3.81	11.250	10.321	10.118	10.084	0.517203	-1.33	0.068	
40186	DD Hya	-5.41	5.88	12.220	11.457	11.241	11.228	0.501771	-0.97	0.013	
41936	TT Cnc	2.42	5.55	11.350	10.330	10.047	9.968	0.563430	-1.57	0.043	
44428	TT Lyn	-1.48	1.75	9.860	8.908	8.655	8.611	0.597429	-1.56	0.017	
45709	RW Cnc	1.05	4.98	11.850	10.677	10.561	10.530	0.547224	-1.67	0.020	
48503	T Sex	2.24	1.56	10.040	9.438	9.268	9.200	0.324706	-1.34	0.044	c
49628	RR Leo	5.01	3.16	10.730	10.021	9.778	9.730	0.452392	-1.60	0.037	
50073	WZ Hya	4.50	5.17	10.900	9.945	9.669	9.610	0.537713	-1.39	0.075	
50289	WY Ant	-0.27	2.51	10.870	9.970	9.744	9.674	0.574341	-1.48	0.059	
53213	AF Vel	0.57	3.19	11.440	10.354	10.079	10.040	0.527414	-1.49	0.250	
55825	W Crt	-1.95	3.43	11.540	10.774	10.590	10.539	0.412015	-0.54	0.040	
56088	TU UMa	0.56	1.68	9.820	8.919	8.740	8.660	0.557658	-1.51	0.022	
56350	AX Leo	-3.10	7.00	12.260	11.302	11.048	10.951	0.726845	-1.72	0.033	
56409	SS Leo	2.50	4.01	11.030	10.259	10.008	9.943	0.626335	-1.79	0.018	
56734	SU Dra	1.27	1.53	9.780	8.898	8.676	8.619	0.660418	-1.80	0.010	
56742	BX Leo	7.73	6.17	11.610	10.889	10.743	10.709	0.362757	-1.28	0.023	c
56785	ST Leo	-0.45	3.47	11.490	10.690	10.480	10.446	0.477990	-1.17	0.038	
57625	X Crt	-3.98	4.50	11.480	10.482	10.213	10.148	0.732842	-2.00	0.027	
58907	IK Hya	1.39	1.62	10.110	9.144	8.863	8.760	0.650371	-1.24	0.061	
59208	UU Vir	2.24	2.91	10.560	9.596	9.436	9.414	0.475597	-0.87	0.018	
59411	AB UMa	0.12	1.94	10.940	9.934	9.678	9.623	0.599593	-0.49	0.022	

Continued on Next Page...

Hipparcos	name	π (mas)	$\Delta\pi$	V	J (mag)	H	K_s	P (day)	[Fe/H]	$E_{(B-V)}$ (mag)	typ
59946	SW Dra	2.24	1.42	10.480	9.594	9.362	9.319	0.569671	-1.12	0.014	
61029	UZ CVn	6.50	7.59	12.120	11.219	10.941	10.885	0.697791	-1.89	0.019	
61031	SV Hya	3.79	2.16	10.530	9.673	9.455	9.366	0.478542	-1.50	0.080	
61225	S Com	5.16	3.66	11.630	10.823	10.678	10.619	0.586585	-1.91	0.019	
61809	U Com	7.40	4.05	11.740	11.186	10.984	10.987	0.292736	-1.25	0.014	c
63054	AT Vir	1.32	3.03	11.340	10.547	10.363	10.332	0.525785	-1.60	0.030	
64875	ST Com	-3.68	3.55	11.460	10.461	10.258	10.186	0.598927	-1.10	0.024	
65063	AV Vir	2.22	4.73	11.820	10.853	10.615	10.566	0.656910	-1.25	0.028	
65344	AM Vir	-1.79	3.17	11.520	10.509	10.253	10.199	0.615063	-1.37	0.067	
65445	AU Vir	0.06	4.99	11.590	11.085	10.918	10.847	0.339616	-1.50	0.028	c
65547	SX UMa	1.90	1.81	10.840	10.288	10.135	10.071	0.307139	-1.81	0.010	c
66122	RV UMa	-0.30	1.85	10.770	10.058	9.854	9.831	0.468069	-1.20	0.018	
67087	RZ CVn	-2.03	2.99	11.570	10.733	10.518	10.478	0.567403	-1.84	0.014	
67227	RV Oct	1.75	2.17	10.980	9.879	9.614	9.526	0.571169	-1.71	0.180	
67354	SS CVn	2.14	3.83	11.840	11.185	10.951	10.936	0.478510	-1.37	0.006	
67976	V499 Cen	-0.01	2.97	11.120	10.225	9.926	9.922	0.521205	-1.43	0.085	
68188	ST CVn	-1.28	4.11	11.370	10.626	10.459	10.449	0.329065	-1.07	0.012	c
68292	UY Boo	1.45	3.00	10.940	9.981	9.755	9.723	0.650889	-2.56	0.033	
68908	W CVn	2.95	2.42	10.550	9.667	9.454	9.371	0.551753	-1.22	0.005	
69759	TV Boo	-0.05	2.09	10.970	10.373	10.282	10.248	0.312557	-2.44	0.010	c
70702	ST Vir	-5.10	5.66	11.520	10.914	10.748	10.671	0.410806	-0.67	0.039	
70751	AF Vir	-9.08	5.23	11.800	10.939	10.769	10.684	0.483735	-1.33	0.023	
71186	RS Boo	1.62	1.91	10.370	9.744	9.559	9.507	0.377339	-0.36	0.012	
72115	TW Boo	-2.23	2.28	11.290	10.407	10.192	10.170	0.532277	-1.46	0.013	
72342	AE Boo	0.33	2.00	10.650	9.974	9.819	9.762	0.314893	-1.39	0.023	c
72444	TY Aps	1.78	3.07	11.850	10.819	10.532	10.456	0.501695	-0.95	0.169	
72691	BT Dra	-1.26	2.08	11.640	10.735	10.478	10.397	0.588673	-1.75	0.010	
72721	XZ Aps	-4.19	5.48	12.380	11.284	11.006	10.923	0.587275	-1.06	0.135	
74556	AP Ser	-0.16	4.32	11.110	10.462	10.305	10.268	0.340805	-1.58	0.042	c
75225	TV CrB	1.89	5.75	11.870	11.037	10.814	10.774	0.584629	-2.33	0.033	
75234	FW Lup	1.58	1.18	9.060	7.995	7.836	7.671	0.484169	-0.20	0.077	
75942	ST Boo	-0.13	1.80	11.010	10.185	9.981	9.930	0.622286	-1.76	0.021	
75982	VY Ser	-0.77	1.99	10.130	9.205	8.944	8.826	0.714101	-1.79	0.040	
76313	CG Lib	-0.50	5.67	11.550	10.437	10.208	10.125	0.306787	-1.19	0.297	c
77663	VY Lib	-1.84	4.04	11.730	10.480	10.174	10.070	0.533941	-1.34	0.192	
77830	AN Ser	-4.47	4.79	10.940	10.096	9.898	9.842	0.522069	-0.07	0.040	
77997	AT Ser	0.18	5.30	11.480	10.533	10.248	10.214	0.746570	-2.03	0.037	
78417	AR Her	2.08	3.25	11.240	10.605	10.413	10.391	0.469981	-1.30	0.013	
79974	RV CrB	3.77	3.21	11.410	10.555	10.418	10.336	0.331593	-1.69	0.039	c
80402	V445 Oph	5.60	5.33	11.050	9.649	9.401	9.262	0.397023	-0.19	0.287	
80853	VX Her	-0.78	2.65	10.690	9.848	9.651	9.590	0.455362	-1.58	0.044	
80990	UV Oct	2.32	1.12	9.500	8.592	8.362	8.297	0.542587	-1.74	0.091	
81238	RW Dra	1.38	2.44	11.710	10.779	10.596	10.622	0.442909	-1.55	0.011	
83244	RW TrA	5.74	3.19	11.400	10.375	10.111	10.059	0.374039	-0.13	0.105	
84233	VZ Her	3.49	2.12	11.480	10.746	10.590	10.496	0.440331	-1.02	0.027	
87681	TW Her	-3.36	2.22	11.280	10.528	10.322	10.239	0.399599	-0.69	0.042	
87804	WY Pav	1.08	6.99	12.180	10.836	10.647	10.553	0.588573	-0.98	0.126	
88064	S Ara	-2.11	3.31	10.780	9.867	9.601	9.560	0.451879	-0.71	0.124	
88402	MS Ara	8.81	5.20	12.070	11.036	10.763	10.664	0.524982	-1.48	0.146	
89326	V675 Sgr	-1.28	2.75	10.330	9.313	9.053	9.003	0.642280	-2.28	0.130	
89372	BC Dra	1.51	1.99	11.600	10.435	10.172	10.096	0.719590	-2.00	0.068	
89450	V455 Oph	-1.47	6.69	12.360	11.395	11.160	11.088	0.453882	-1.07	0.144	
90053	IO Lyr	-0.84	2.95	11.850	10.841	10.591	10.538	0.577121	-1.14	0.074	
91634	CN Lyr	-3.91	2.52	11.480	10.282	10.055	9.919	0.411383	-0.58	0.178	
92244	V413 CrA	-1.75	3.26	10.600	9.497	9.248	9.148	0.589343	-1.26	0.075	
93476	MT Tel	1.17	1.46	8.980	8.323	8.176	8.076	0.316900	-1.85	0.038	c
94134	XZ Dra	2.28	1.20	10.250	9.398	9.221	9.148	0.476497	-0.79	0.062	
94869	BK Dra	0.67	1.52	11.190	10.336	10.124	10.071	0.592076	-1.95	0.052	
95497	RR Lyr	3.79	0.19	7.760	6.759	6.546	6.489	0.566839	-1.39	0.030	

Continued on Next Page...

Hipparcos	name	π (mas)	$\Delta\pi$	V	J (mag)	H	K_s	P (day)	[Fe/H]	$E_{(B-V)}$ (mag)	typ
95702	BN Vul	3.56	3.08	11.020	9.138	8.793	8.677	0.594138	-1.61	0.173	
96101	V440 Sgr	-0.09	3.43	10.340	9.402	9.153	9.082	0.477479	-1.40	0.085	
96112	XZ Cyg	1.83	1.01	9.680	8.990	8.793	8.722	0.466610	-1.44	0.096	
96581	BN Pav	6.43	6.05	12.600	11.593	11.344	11.279	0.567117	-1.32	0.073	
98265	BP Pav	3.50	6.34	12.540	11.648	11.386	11.366	0.527128	-1.48	0.059	
101356	V341 Aql	-4.86	5.62	10.850	9.886	9.687	9.606	0.578017	-1.22	0.086	
102593	DX Del	0.40	1.94	9.940	9.048	8.746	8.685	0.472619	-0.39	0.092	
103364	UY Cyg	2.55	2.91	11.110	10.060	9.805	9.777	0.560714	-0.80	0.129	
103755	RV Cap	0.85	3.82	11.040	9.703	9.717	9.753	0.447698	-1.61	0.041	
104613	V Ind	1.09	2.06	9.960	9.274	9.028	8.985	0.479604	-1.50	0.043	
104930	SW Aqr	-3.93	4.09	11.180	10.413	10.142	10.057	0.459299	-1.63	0.076	
105026	Z Mic	0.69	3.53	11.650	10.478	10.179	10.112	0.586925	-1.10	0.094	
105285	YZ Cap	4.62	2.78	11.300	10.532	10.437	10.429	0.273461	-1.06	0.063	c
106645	SX Aqr	2.42	3.58	11.780	10.973	10.689	10.639	0.535712	-1.87	0.048	
106649	RY Oct	-1.87	4.88	12.060	11.118	10.917	10.859	0.563475	-1.83	0.113	
107078	CG Peg	3.16	2.49	11.180	10.216	10.007	9.970	0.467133	-0.50	0.074	
107935	AV Peg	2.88	2.44	10.500	9.609	9.406	9.346	0.390378	-0.08	0.067	
108057	SS Oct	9.09	3.32	11.910	10.041	9.835	9.752	0.621852	-1.60	0.285	
108839	BV Aqr	7.24	4.15	10.900	10.228	10.017	10.075	0.363653	-1.42	0.034	
111839	RZ Cep	0.60	1.48	9.470	8.168	7.959	7.883	0.308688	-1.77	0.078	c
112994	BH Peg	-0.72	2.38	10.460	9.385	9.114	9.067	0.640991	-1.22	0.077	
115135	DN Aqr	-1.08	2.82	11.200	10.158	9.934	9.900	0.633757	-1.66	0.025	
115870	RV Phe	1.75	4.71	11.940	11.106	10.828	10.768	0.596416	-1.69	0.007	
116664	BR Aqr	0.71	3.48	11.420	10.648	10.421	10.370	0.481872	-0.74	0.027	
116942	VZ Peg	4.89	3.75	11.900	11.219	11.059	11.010	0.306493	-1.80	0.045	c
116958	AT And	-2.25	1.85	10.710	9.478	9.181	9.087	0.616917	-1.18	0.110	

The stars are those listed by Fernley et al. (1998) and we have generally adopted their V magnitudes and $[\text{Fe}/\text{H}]$ values. The parallaxes and their standard errors are from the revised Hipparcos catalogue (van Leeuwen 2007). Details regarding the formation of the table, particularly the derivation of mean JHK_s values from the single 2MASS values, are given in Appendix B³. DH Peg, which is in the Fernley et al. list, has been omitted because its status is doubtful. It may be a dwarf Cepheid (Fernley et al. 1990). There are a number of other stars which are listed as RR Lyrae stars in the Hipparcos catalogue. In some cases this classification is incorrect or doubtful. For instance DX Cet is actually a δ Sct star (Kiss et al. 1999). This star is, in fact, of special interest as having a parallax with a small percentage error and falling on the PL relation for fundamental mode δ Sct pulsators (van Leeuwen 2007). A discussion of stars whose classification as RR Lyrae type is probably incorrect or uncertain will be given elsewhere (Kinman, in preparation). The parallaxes and magnitudes of the very few Hipparcos stars which are probably RR Lyraes and were not in the Fernley list are such that they would make no significant contribution to the results given in this paper. It seemed better therefore to omit them and thus, for instance, have the homogeneous set of $[\text{Fe}/\text{H}]$ results given by Fernley et al. The reddenings, $E(B - V)$, listed are the means of the two values discussed in section 3.2. These two values agree closely, the maximum difference (0.06 mag) being that for BN Vul, a star at low galactic latitude. For RZ Cep, which is also close to the plane, the difference is 0.03 mag. All other stars show smaller differences.

We assume in the following that,

$$A_V = 3.06E(B - V)$$

and with data on the 2MASS system we adopt,

$$A_J = 0.764E(B - V),$$

$$A_H = 0.450E(B - V),$$

$$A_{K_s} = 0.285E(B - V).$$

These values are from Laney & Stobie (1993) as adjusted for K_s by Gieren et al. (1998). The table indicates the c-type variables. The fundamental periods of these stars were obtained by multiplying the observed period by 1.342.

3.2 Results

The revised Hipparcos parallax of RR Lyrae is $\pi = 3.46 \pm 0.64$. Benedict et al. (2002a) found $\pi = 3.82 \pm 0.20$ from HST observations. In the present paper we adopt a weighted mean of these values, $\pi = 3.79 \pm 0.19$. This takes the quoted standard errors, each of which has their own uncertainties, at their face value. Giving higher weight to the globally-determined revised Hipparcos value would increase the derived brightness of the star by ≤ 0.2 mag. We then obtain the following absolute magnitudes after adding a Lutz-Kelker correction of -0.02 which was calculated on the same basis

³ Since our analysis of the RR Lyrae data was completed, Sollima et al. (2007) have published mean J, H, K_s data for RR Lyrae itself. They measured against 2MASS stars as standards and found: 6.74 ± 0.02 , 6.60 ± 0.03 and 6.50 ± 0.02 . The values we derived (Table 1) are 6.76, 6.55 and 6.49. The Sollima et al. results provide a useful confirmation of our procedure. Since their value of K_s is negligibly different from our value we have kept our value in the following.

as that adopted by Benedict et al.:

$$M_V = +0.54, M_{K_s} = -0.64,$$

each with standard error of ± 0.11 . In deriving the above figures we have adopted the data for RR Lyrae in Table 1. The reddening, $E(B - V) = 0.030$, given there agrees with the value derived directly from its parallax distance and the Drimmel et al. (2003) formulation discussed below (0.031).

There are 142 stars, including RR Lyrae itself, in Table 1. Reduced parallax solutions (see, e.g. Feast 2002) were carried out for this group of stars. The reddenings were estimated for each star using the Drimmel et al. (2003) three-dimensional Galactic extinction model, including the rescaling factors that correct the dust column density to account for small-scale structure seen in the DIRBE data but not described explicitly by the model. Two initial estimates were made of the distance of a star using the tabulated mean K_s or V magnitudes and preliminary PL(K_s) or $M_V - [\text{Fe}/\text{H}]$ relations, both of which correspond to an LMC modulus of ~ 18.5 . The results were iterated (see e.g. Whitelock et al. (2008)). The values of $E(B - V)$ tabulated and used are the means of the final results from K_s and V .

A reduced parallax solution of eq. 1 for the 142 stars and adopting $a = 0.214$, then leads to:

$$M_V = +0.54,$$

at the mean metallicity of the sample ($[\overline{\text{Fe}/\text{H}}] = -1.38$). Similarly, reduced parallax solutions lead to,

$$M_{K_s} = -0.63$$

at the mean $\log P$ of the sample ($\overline{\log P} = -0.252$), adopting a PL(K_s) slope of -2.41 as in eq. 4. The standard error of these derived absolute magnitudes is ± 0.10 . (Note that no Lutz-Kelker correction is required in this case). These results are essentially identical to those for RR Lyrae itself and indeed the solution is completely dominated by this one star. Omitting RR Lyrae leads to solutions with very large standard errors. In the following we simply use the results based on RR Lyrae alone, but using the full set of stars would obviously make no difference.

We then find,

$$b = 19.39 - \text{Mod}(\text{LMC}) = +0.84 \pm 0.11$$

for eq. 1 with $a = 0.214$ as in eq. 2. This gives absolute magnitudes brighter by 0.16 ± 0.12 than those given by eq. 2 with an LMC modulus of 18.39 ± 0.05 . The standard error does not take into account the scatter about the $M_V - [\text{Fe}/\text{H}]$ relation, which can be substantial (see e.g. Gratton et al. fig. 19.). This result is consistent with the prediction of Catalan & Cortés (2008) that RR Lyrae is over luminous for its metallicity by 0.06 ± 0.01 mag compared with the average members of this class. Note that if we adopted their preferred reddening for RR Lyrae we would reduce the over luminosity implied by our result from 0.16 ± 0.12 to 0.12 ± 0.12 .

Main-sequence fitting procedures (Gratton et al. 2003) lead to $b = +0.89 \pm 0.07$. However, other work (e.g. Salaris et al. 2007) has suggested a smaller distance modulus for 47 Tuc, a cluster on which the result of Gratton et al. partly depends. Thus their value of b may need increasing slightly. The statistical parallaxes from Popowski & Gould (1998) lead to a value of $b = +1.10 \pm 0.12$, that is to absolute magnitudes 0.10 ± 0.12 fainter than eq. 2.

The parallax data on RR Lyrae leads to a constant term in eq. 3 of -1.12 . This is 0.07 mag brighter than the value given by Sollima et al. which was based on the HST paral-

Table 2. Data for Type II Cepheids: Hipparcos Parallaxes

	VY Pyx	κ Pav
$\log P$	0.093	0.959
$[Fe/H]$	-0.44	0.0
B	7.85	4.98
V	7.30	4.35
I		3.67
J	6.00	3.17
K_s	5.65	2.78
$E(B - V)$	0.049	0.017
π	5.00	6.51
σ_π	0.44	0.77
Mod	6.59	5.93
σ_{Mod}	0.19	0.26
LK	-0.06	-0.12
M_B	+1.09	-1.14
M_V	+0.54	-1.86
M_I		-2.41
M_{K_s}	-0.92	-3.27

lax of RR Lyrae alone and a slightly different K_s magnitude. Following the discussion in Sollima et al. (2006), which takes into account metallicities of the LMC variables, the parallax result leads to a distance modulus of the LMC which is 0.22 ± 0.14 larger than that deduced from the classical Cepheids (18.39 ± 0.05). A main uncertainty in the Cepheid result was in the metallicity correction adopted, and the RR Lyrae parallax result may indicate that this was overestimated. However, the errors are such that within the uncertainties the classical Cepheids and RR Lyrae variable scales are substantially in agreement.

4 THE TYPE II CEPHEIDS

4.1 Trigonometrical parallaxes

The relevant data for the two Cepheids on our programme are collected in Table 2. The metallicity of VY Pyx is from Maas et al. (2007). The value quoted for κ Pav is from Luck & Bond (1989). Both stars are comparatively metal-rich. The BV photometry of VY Pyx is from Sanwal & Sarma (1991), whilst J and K_s are single 2MASS values. In view of the low visual amplitude of VY Pyx ($\Delta V = 0.27$), these should be close to mean values. The magnitudes, light curve and period agree satisfactorily with the Hipparcos photometry (ESA 1997). For κ Pav the intensity mean B , V and I were derived from the literature cited in Table 3, with I in the Cousins system. J , K_s for this star are from the intensity means given in section 4.2.2 transformed to the 2MASS system using the relations derived by Carpenter (2001 as updated on the 2MASS Web page). The reddenings for both stars were estimated on the Drimmel et al. (2003) model described in section 3.2, with distances adopted from the revised Hipparcos parallaxes ($\pi \pm \sigma_\pi$) which are also listed. The distance moduli (Mod) and their uncertainties come directly from the parallaxes. The Lutz-Kelker (LK) corrections needed in deriving the absolute magnitudes are calculated on the same system as used for RR Lyrae (section 3). In discussing the various absolute magnitudes listed we shall use for their standard errors the values derived for

the distance moduli. It should be borne in mind that these may be slightly underestimated due to any uncertainty in photometry, reddening and Lutz-Kelker correction.

There are other stars classified as CephIIs in the Hipparcos catalogue in addition to κ Pav and VY Pyx, but their σ_π/π values are relatively high and in some cases it is uncertain whether they belong to the CephII class. We have therefore not attempted to use these stars.

4.2 Pulsation parallaxes

4.2.1 The Projection factor, p

The Baade-Wesselink method for radius determination has seen only limited use for CephIIs, even at optical wavelengths, and table 2 in Balog et al. (1997) suggests that such results as have been reported are somewhat inconsistent with each other.

For classical Cepheids, the reasons for using IR photometry in determining pulsation parallaxes or Baade-Wesselink radii have been given by Laney & Stobie (1995 henceforth LS95), and by Gieren, Fouqué & Gomez (1997), among others. This technique has not been used previously in determining radii, luminosities, etc. for CephIIs, except for a few preliminary results given by Laney (1995). Whilst modern pulsation parallaxes are often of high internal consistency, it has been difficult to estimate possible systematic uncertainties. Significant progress in dealing with such systematic uncertainties has become possible since the advent of reasonably accurate parallaxes for nearby classical Cepheids (Benedict et al. 2002b, 2007, van Leeuwen et al. 2007), as these allow a particular pulsation parallax method to be calibrated empirically.

Several recent papers (Merand et al. 2005, Groenewegen 2007, Nardetto et al. 2007, Fouqué et al. 2007) have tackled the determination of the projection factor (p -factor), which has long been one of the principal sources of uncertainty in pulsation parallaxes. Other papers have discussed angular diameter measurements and the surface-brightness colour relation, but these are not as directly relevant to the method used here, as the radii derived in this paper have been calculated using the technique described in Balona (1977), where the surface-brightness coefficient is a free parameter. Conversion from radii to luminosities uses a methodology described below, and is in effect included in the calibration of the p -factor.

As in LS95, solutions have been derived with a modified version of Luis Balona's software which allows for a non-negligible amplitude, and where photometric magnitudes and colours, as well as radial velocities, are assigned individual errors. All radii used were derived using K as the magnitude and $V - K$ or $J - K$ as the colour, as this approach was shown to be free of serious phase-dependent systematic error by LS95. These authors also show that inclusion or exclusion of the rising branch has a negligible systematic effect on the derived radii, although excluding the rising branch increases the uncertainty in the results. Here J, K are on the SAAO system (see below, Appendix A). Adopted radii are the means of the $(K, V - K)$ and $(K, J - K)$ values. The adopted formal error in the radius is derived by taking the square root of the mean of the squares of the individual errors in the $(K, V - K)$ and $(K, J - K)$ radii.

Table 3. Pulsation Parallax solutions for Classical Cepheids and κ Pav

Star	Period	$\langle K_o \rangle$	$\langle J_o \rangle$	$\langle V_o \rangle$	R_1	R_2	M_K	π_1	π_2	p
δ Cep	5.3662475	2.295	2.678	3.667	41.3 ± 1.0	42.5 ± 1.0	-4.86	$3.71 \pm .12$	$3.72 \pm .09$	$1.27 \pm .05$
X Sgr	7.012675	2.453	2.833	3.819	49.3 ± 1.6	47.3 ± 1.4	-5.16	$3.17 \pm .14$	$3.01 \pm .09$	$1.20 \pm .06$
β Dor	9.842578	1.947	2.405	3.616	62.1 ± 1.7	63.0 ± 1.0	-5.64	$3.26 \pm .14$	$3.04 \pm .07$	$1.18 \pm .06$
ζ Gem	10.14992	2.128	2.605	3.884	62.7 ± 1.7	65.4 ± 1.6	-5.67	$2.74 \pm .12$	$2.76 \pm .07$	$1.28 \pm .06$
l Car	35.54327	1.046	1.639	3.225	162.3 ± 4.0	165.7 ± 3.0	-7.59	$2.03 \pm .16$	$1.87 \pm .04$	$1.17 \pm .10$
κ Pav	9.0880	2.795	3.201	4.291	26.5 ± 0.8	26.3 ± 0.6	-3.81	$6.51 \pm .77$	$4.78 \pm .13$	$0.93 \pm .11$

The columns contain: (1) star name, (2) period in days, (3,4,5) intensity mean magnitudes corrected for reddening ($\langle K_o \rangle$, $\langle J_o \rangle$ in the SAAO system), (6,7) radii in solar units derived from K , $J - K$ (R_1) and K , $V - K$ (R_2) with $p = 1.27$ (8) the trigonometrical parallax and its s.e. (9) pulsation parallax and its (internal) s.e. (11) p . The errors of the mean radius and the trig. parallax have been added in quadrature for σ_p .

References: δ Cep, 1,2,3,A,B,C; X Sgr, 1,4,5,6, D-N; β Dor, 7-10, O,P; ζ Gem, 1,3,13,A,C,Q; l Car, 7,9,10,11,M,R; κ Pav, 7,9,13,15,16,P.

Optical Photometry references: (1) Moffett & Barnes 1984, (2) Barnes et al. 1997, (3) Kiss 1998, (4) Shobbrook 1992, (5) Arellano Ferro et al. 1998, (6) Berdnikov & Turner 2001, (7) Dean et al. 1977, (8) Pel 1976, (9) Dean 1981, (10) Shobbrook 1992, (11) Bersier 2002, (12) Szabados 1981, (13) Dean 1977, (14) Berdnikov 1997, (15) ESA 1997, (16) Cousins & Lagerweij 1971.

Radial Velocity references: (A) Bersier et al. 1994, (B) Butler 1993, (C) Kiss 1998, (D) Moore 1909, (E) Duncan 1932, (F) Stibbs 1955, (G) Feast 1967, (H) Lloyd Evans 1968, (I) Lloyd Evans 1980, (J) Barnes et al. 1987, (K) Wilson et al. 1989, (L) Sasselov & Lester 1990, (M) Bersier 2002, (N) Mathias et al. 2006, (O) Taylor & Booth 1998, (P) Wallerstein et al. 1992, (Q) Gorynya et al. 1998, (R) Taylor et al. 1997.

The first necessary step is to derive an appropriate value of the p -factor for the *specific method used here*. Our radius-determination methodology is different from those used by Merand et al. (2005), Groenewegen (2007) and Nardetto et al. (2007), and the radial velocities (selected from the literature) are not based on a single selected line, as described by Nardetto et al. (2007).

As a first approximation, $p = 1.27$ (Merand et al. 2005, Groenewegen 2007) was adopted, and radii were calculated for five of the classical Cepheids in table 2 of van Leeuwen et al. (2007). Polaris has a limited, variable amplitude and we are unaware of suitable data for an accurate radius solution. For FF Aql the possible influence of a binary companion and the low quality of the JHK data were enough to drop it from the list. The other stars in the van Leeuwen et al. list have higher σ_π/π than our five stars.

For the remaining five stars, the (K , $V - K$) and (K , $J - K$) radii were calculated with $p = 1.27$, then converted into luminosities. This was done using the tables given in Hindsley & Bell (1990) to establish the K -band absolute magnitudes for a star of one solar radius and the appropriate dereddened $V - K$ and $J - K$ colours, then taking the mean. As discussed in LS95, the K surface brightness as a function of $J - K$ or $V - K$ is very insensitive to surface gravity or microturbulence, which means that neither the radius solution nor the derived luminosity is significantly affected by assumptions about mean or time-varying values for these quantities in the stellar atmosphere. A similar procedure was followed for κ Pav, the only CepII which has good JHK and radial velocity data and a usable parallax measurement – though this is of lower quality than for the five classical Cepheids. Dereddening was done using the reddening coefficients derived by Laney & Stobie (1993), and $BVIc$ reddenings for each star as calibrated recently by Laney & Caldwell (2007), using metal abundances from the tables in that paper, or for κ Pav the value from Luck & Bond (1989). The resulting small uncertainty in the colours has only a small effect on the K surface brightness, as it is only a weak function of either $V - K$ or $J - K$. Figs. 1-6 show the match of radius displacements calculated from the

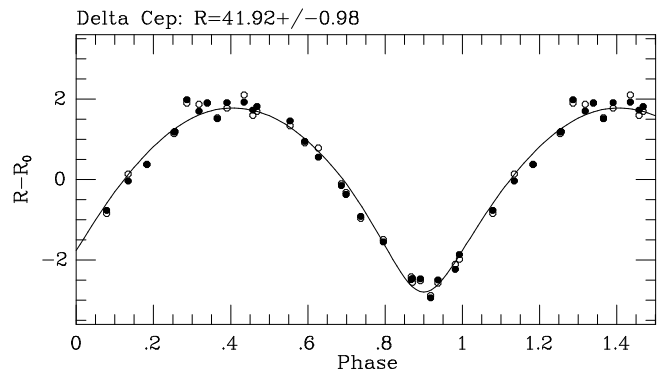


Figure 1. Radius displacements for δ Cep calculated from the K , $J - K$ (open circles) and K , $V - K$ (filled circles) radius solutions and photometry, vs. the integrated radial velocity curve (solid line). A projection factor of $p = 1.27$ was used.

radius solution and VJK photometry to the integrated radial velocity curve. As would be expected from LS95, there are no serious phase anomalies or discrepancies. Any serious problems with shock waves, etc. that distorted the solutions should appear in these diagrams, but there is no real sign of such an effect – even for X Sgr (Sasselov & Lester 1990, Mathias et al. 2006) or κ Pav. For any other value of the projection factor, the curves would appear identical to those shown except that the vertical scale would be slightly different.

In all cases, it was necessary to establish the phase and period behaviour of the star, so that there were no systematic shifts between the phases or zero-points of the optical photometry, infrared photometry and radial velocities. For X Sgr, it was also necessary to redetermine the orbital velocity curve, in view of the doubts expressed by Mathias et al. (2006). All velocities in the literature for this star, including the most recent, appear to be consistent with the orbital period determined by Szabados (1990), and it proved possible to separate the orbital and pulsational velocities effectively

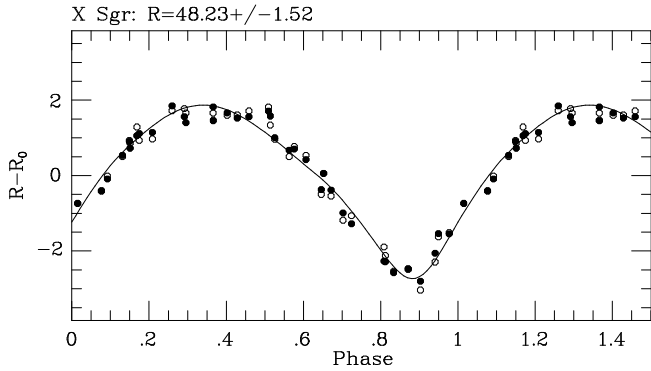


Figure 2. As Fig. 1, but for X Sgr.

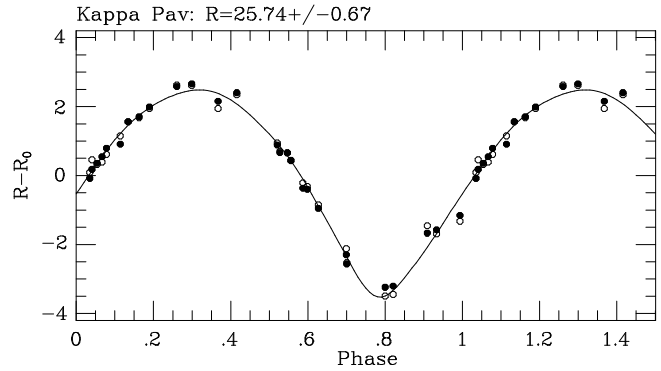


Figure 6. As Fig. 1, but for κ Pav.

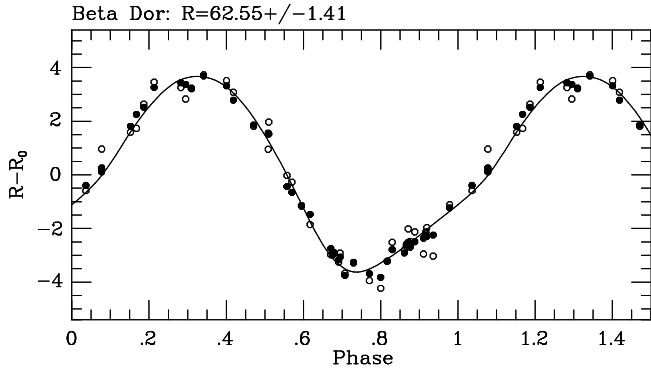


Figure 3. As Fig. 1, but for β Dor.

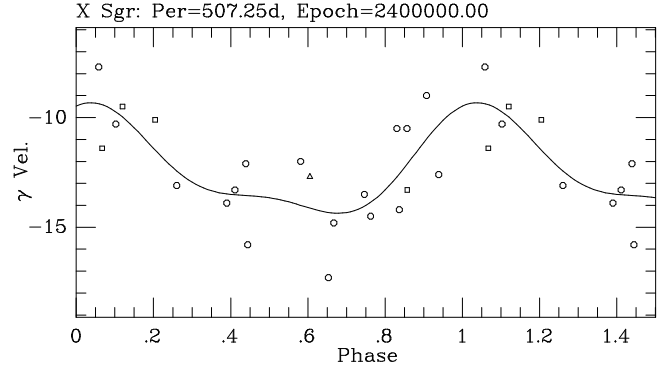


Figure 7. Gamma velocities for X Sgr, phased according to the ephemeris and period of Szabados (1990). The squares represent data from Bersier (2002) and Sasselov & Lester (1990). The triangle is the value from Mathias et al. (2006).

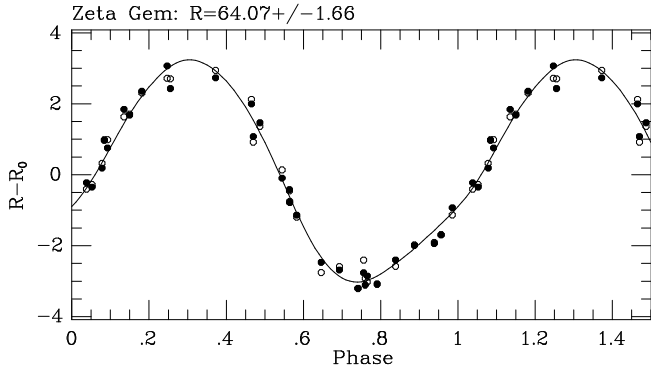


Figure 4. As Fig. 1, but for ζ Gem.

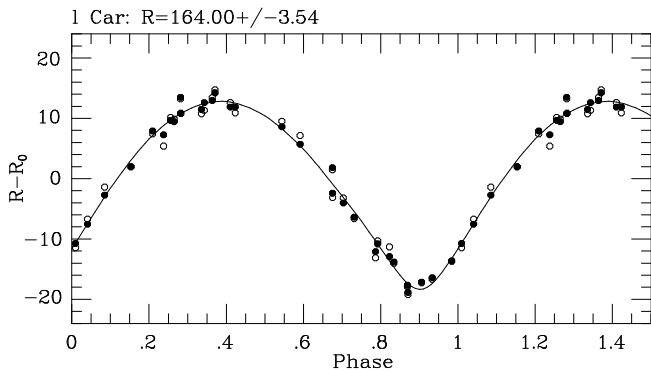


Figure 5. As Fig. 1, but for l Car.

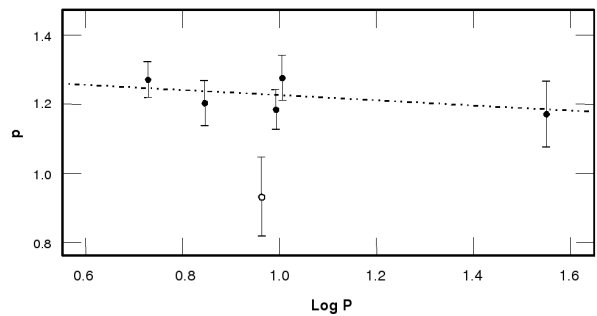


Figure 8. The projection factor, p , plotted against $\log P$ for the classical Cepheids, δ Cep, X Sgr, β Dor, ζ Gem, and l Car (filled circles) and the CephII κ Pav (open circle). The line shows the trend of p with period suggested by Nardetto et al. (2007), but adjusted to the zero-point given by the five classical Cepheids.

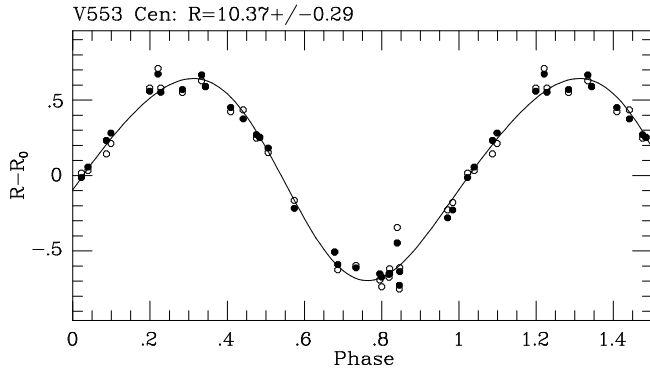


Figure 9. As Fig. 1, but for V553 Cen and adopting $p = 1.23$.

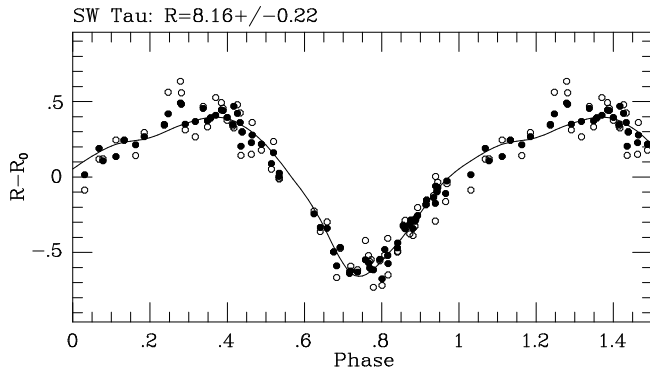


Figure 10. As Fig 1, but for SW Tau and adopting $p = 1.23$.

(Fig. 7), though better data are desirable. The *JHK* data used are listed in Appendix A.

Radii, luminosities and pulsation parallaxes for the five classical Cepheids and κ Pav, derived as above for $p = 1.27$, are given in Table 3, together with the sources for the optical photometry and radial velocities. Also in this table are the trigonometrical parallaxes from van Leeuwen et al. (2007) and the present paper. Requiring that the p -factor for each star be adjusted to produce agreement between the pulsation and trigonometric parallaxes leads to the empirical p -factors for each star listed in Table 3 together with the associated errors due to the uncertainties in both the radius and the trigonometric parallax. These lead to the empirical p -factor for each star listed in the table together with the associated errors due to uncertainty in the radius and in the parallax. These values of p are plotted against $\log P$ in Fig. 8. For all 5 classical Cepheids, the derived p -factor falls within a narrow range, and the mean is 1.22 ± 0.02 , weighting the stars equally. An average, weighted according to the inverse square of the error, gives 1.23 ± 0.03 where the weight of *l* Car has been set to one and its error has been divided by the square root of the sum of the weights for all five stars. A trend with period may be present, as claimed in Nardetto et al. (2007), though our sample is too small to derive a useful, statistically significant value of a term in $\log P$. If we assume that there is a $\log P$ term of -0.075 (given by Nardetto et al. as appropriate for velocities based on a mix of lines of varying depth), the weighted intercept at $\log P = 1.0$ is 1.23 ± 0.03 .

The derived p -factor for κ Pav, on the other hand, is

strikingly discrepant, so low as to be physically unrealistic, especially given that the colours and surface gravity are in reasonable accord with those given for classical Cepheids by Laney & Stobie (1994) and Fernie (1995) respectively, while the metallicity is solar (Luck & Bond 1989) and the radius displacement diagram (Fig. 6) resembles those of the 5 classical Cepheids. However, the parallax for this star is more uncertain than for the five classical Cepheids, and the derived p -factor is in fact only about 2σ from the weighted mean of the 5 classical Cepheids. A p -factor of 1.23 was adopted for all three Cepheids considered here⁴. Details of the radius and luminosity determinations follow. Magnitudes, radii, absolute magnitudes and other relevant data are given in Tables 4 and 5.

4.2.2 κ Pav

The best-fitting period for the IR data in Table A1 (JD 2445928-2447769) was 9.0814 d, and the scatter around a low-order (2 to 5) Fourier fit to the resulting magnitudes and colours was about 0.009-0.011 mag. This is rather higher than normal for such a bright star, and suggests a modest amount of phase jitter may have been present.

Contemporaneous radial velocity data were available in the literature (Wallerstein et al. 1992), covering almost exactly the same range of Julian dates. A modest number of velocities with slightly later JD were shifted into phase agreement at the adopted period. The light curve of κ Pav is known for sudden changes (Wallerstein et al. 1992), so a need for phase adjustments is not surprising.

The sources of the visual photometry are given in Table 3. All datasets have been phased at their appropriate periods, then shifted into phase and zero-point agreement with Dean et al. (1977) and Dean (1981). This composite dataset was used to derive a 6th order Fourier fit to the *V* light curve, with maximum light in *V* set to phase 0. None of the optical photometry data sets was contemporary with the infrared data. Derived periods and epochs were:
 2440140.119 + 9.0947E (Cousins & Lagerweij)
 2441959.49903 + 9.08352E (Dean et al., Dean)
 2448164.8647 + 9.092405E (Shobbrook, Hipparcos, Berdnikov, Berdnikov & Turner)

A *V* magnitude was then calculated for each infrared observation, using an epoch for the IR data which ensured that a Fourier fit to the *V* - *K*, and *J* - *K* data gave phases for minimum light in agreement with those for *B* - *V* and *V* - *I*, a technique for phase alignment validated by LS95. The resulting (*K*, *J* - *K*) and (*K*, *V* - *K*) radii agree within less than one percent, and there are no significant phase-dependent anomalies (Fig. 6).

$E(B - V) = 0.017 \pm 0.022$ was derived from the *B* - *V* and *V* - *I* magnitude means (and the solar metallicity given by Luck & Bond (1989)), using the Cousins reddening method as re-calibrated by Laney & Caldwell (2007). While this method has not been specifically calibrated for Cepheids, κ Pav falls into much the same range in temperature, surface gravity and metallicity as classical Cepheids. This reddening is virtually the same as that derived by the Drimmel method (0.019). The reddening value is in any event not critical -

⁴ See also the discussion in section 5.1.

Table 4. Pulsation Parallax Results for Type II Cepheids

Star	Per	$\langle K_o \rangle$	$\langle H_o \rangle$	$\langle J_o \rangle$	$\langle V_o \rangle$	R_1	R_2	D
SW Tau	1.583565	7.887	7.931	8.147	8.800	8.02 ± 0.27	8.03 ± 0.15	$732 \pm 20 \pm 16$
V553 Cen	2.060464	6.878	6.963	7.290	8.455	10.53 ± 0.33	10.20 ± 0.25	$541 \pm 15 \pm 12$
κ Pav	9.0902	2.795	2.863	3.201	4.291	26.48 ± 0.78	26.32 ± 0.62	$204 \pm 5 \pm 4$

The columns are: (1) star name, (2) period in days (for κ Pav this is the mean of the three periods used for the optical photometry), (3,4,5,6) intensity mean magnitudes with the infrared values on the SAAO system, (7,8) radii in solar units from, $K, J - K$ (R_1) and $K, V - K$ (R_2), (9) distance in pc based on a mean of R_1 and R_2 and with $p = 1.23$ (the first standard error reflects the uncertainty in the derived radius, the second the uncertainty in p).

Table 5. Data for Type II Cepheids: Pulsation Parallaxes

	κ Pav	V553 Cen	SW Tau
$\log P$	0.959	0.314	0.200
$[Fe/H]$	0.0	+0.24	+0.22
B	4.98	9.15	10.32
V	4.35	8.46	9.66
I	3.67	7.76	8.94
K_s	2.78	6.86	7.95
K_W	2.55	6.63	7.73
$E(B - V)$	0.017	0.00	0.282
Mod	6.55	8.67	9.32
σ_{Mod}	0.07	0.08	0.08
M_B	-1.64	+0.48	-0.15
M_V	-2.25	-0.21	-0.53
M_I	-2.91	-0.90	-0.88
M_{K_s}	-3.77	-1.80	-1.46

it affects the luminosity and distance determinations *only* through the weak dependence of K surface brightness on the dereddened $V - K$ and $J - K$ colour indices.

Dereddened $V - K$ and $J - K$ colours were used to calculate the surface brightness at K as described above, using $\log g$ of 1.2 (Luck & Bond 1989), and converted to absolute magnitudes at V, J and K using the mean radius and the dereddened empirical colours. 2MASS J, H and K_s , absolute magnitudes were calculated using the transformations on the 2MASS website, as they also were for V553 Cen and SW Tau, below.

4.2.3 V553 Cen

The period behaviour is simpler than for κ Pav, and seems adequately described by:

$$2448437.1154 + 2.060464E(2444423-2450364) \\ 2443108.6572 + 2.060608E(2440700-2443686)$$

These phases were adopted for the IR photometry (Table A1), for optical photometry by Wisse & Wisse (1970), Lloyd Evans et al. (1972), Dean et al. (1977), Dean (1981), Eggen (1985), Diethelm (1986), Gray & Olsen (1991), ESA (1997), Berdnikov & Turner (1995) and Berdnikov (1997), and for radial velocities by Wallerstein & Gonzalez (1996) and Lloyd Evans et al. (1972). All optical photometry was adjusted in zero point to match Dean et al. (1977) and Dean (1981), and the radial velocities to match Wallerstein and Gonzalez.

The mean $E(B - V)$ for solar metallicity and a microturbulence of 2.5 km s^{-1} (Wallerstein and Gonzalez 1996)

is 0.00 ± 0.02 from 54 observations with $B - V$ and $V - I$. These authors also derive $\log g \sim 1.8$. The Drimmel procedure gives $E(B - V) = 0.08$.

The derived ($K, J - K$) and ($K, J - K$) radii agree within the errors, and the lack of significant phase-dependent anomalies can be seen in Fig. 9.

4.2.4 SW Tau

The period seems essentially constant at 1.583565d over the relevant interval, with an epoch of 2445013.2696 for maximum light in V . Optical photometry has been taken from Barnes et al. (1997), Moffett & Barnes (1984), and Stobie & Balona (1979), and the zero-point shifted to match Stobie & Balona. For $B - V$ and $V - I$ magnitude means of 0.653 and 0.796 on the Cousins system, with $[Fe/H] = +0.2$, microturbulence of 3.0 km s^{-1} (Maas et al. 2007), $E(B - V)$ is 0.282 ± 0.031 . $\log g$ from Maas et al. is about 2.0. The Drimmel procedure gives $E(B - V) = 0.26$.

IR data for SW Tau on the CIT system was taken from Barnes et al. (1997) and transformed to the Carter system by the formulae given in Laney & Stobie (1993). This was then combined with the SAAO JHK observations, and matched to the SAAO zero point. As would be expected, the resulting shifts were small.

Radial velocities used are those from Gorynya et al. (1998) and from Bersier et al. (1994).

The derived ($K, J - K$) and ($K, J - K$) radii agree within the errors, and the lack of significant phase-dependent anomalies can be seen in Fig. 10.

5 DISCUSSION

5.1 κ Pav

The trigonometrical and pulsational parallaxes of κ Pav are 6.51 ± 0.77 and 4.90 ± 0.17 , a difference of 1.61 ± 0.79 . This 2σ difference is sufficiently large to raise some concerns. The Hipparcos result is from a type 3 solution. In such a solution account is taken of possible variability induced motion. Further investigation shows evidence (Fig. 11) for a magnitude dependence difference between the DC and AC Hipparcos magnitudes. These magnitude systems and the interpretation of differences between them are described in the Hipparcos catalogue (ESA 1997). The results for κ Pav suggest the presence of a close companion consistent with the need for a type 3 solution. Given the method of reduction employed, the revised Hipparcos parallax should be reliable within the quoted uncertainty.

The possibility that κ Pav was a spectroscopic binary was suggested by Wallerstein et al. (1992) from a comparison of their work with much earlier observations. There is, however, no evidence of short period variations in γ velocity in their data which extended over a considerable time span (JD 2445860-2448283) or the additional data we have used. The five-colour photometry of Janot-Pacheco (1976) shows no evidence of a bright companion. The present work provides internal checks on the possibility of a bright companion. A bright red companion would produce abnormally low surface brightness coefficients in the $(K, J - K)$ and, especially, the $(K, V - K)$ solutions. A companion of similar colour to the variable would affect the two solutions more equally. In fact, these two surface brightness coefficients are slightly higher for κ Pav than the other two Cepheids in the programme, though not significantly so. A blue companion would tend to make the $(K, V - K)$ radius smaller than the $(K, J - K)$ one. The $(V, B - V)$ radius would be smaller still and have an unusually large surface brightness coefficient as seen in the classical Cepheid binary KN Cen (LS95). In κ Pav there is no significant difference between the $(K, V - K)$ and $(K, J - K)$ radii. The $(V, B - V)$ radius is smaller by 13 percent. This is a marginal effect and indicates that any blue companion has a relative brightness considerably fainter than in the case of KN Cen.

Thus, in summary, no serious anomalies were found in the pulsation parallax analysis besides the problem of phase shifts. However, some caution is necessary in discussing this star. In the following, we discuss the results separately for the two estimates of the parallax.

5.2 Infrared period-luminosity relations

Table 6 lists the differences of the parallax based absolute magnitudes from the $PL(K_s)$ relation (eq. 4). We adopt $c = -1.0$ corresponding to an LMC modulus of 18.39. Besides the Cepheid stars, Table 6 lists, in addition, the results for RR Lyrae. As already noted, Matsunaga et al. (2006) suggested that the RR Lyrae variables lay on the same $PL(K_s)$ relation as the Cepheids and this suggestion was strengthened by the work of Sollima et al. (2006). Two standard errors are given, σ_1 is the value derived from the parallax solution and σ_2 combines this in quadrature with the scatter in the $PL(K_s)$ relation as given by Matsunaga et al. (2006) (0.14). This latter value is an upper limit to the intrinsic scatter of the Matsunaga et al. relation since it includes uncertainties in the moduli of the globular clusters they used etc. The first part of Table 6 shows the results from the trigonometrical parallaxes and the second part the results from the pulsation parallaxes.

Given the uncertainties in the trigonometrical parallaxes, the results in the first part of Table 6 show satisfactory agreement with the predictions of the infrared PL relation. The two short period stars with pulsation parallaxes (SW Tau, $P = 1.58$; V533 Cen, $P = 2.06$) agree closely with predictions. This agreement is sufficiently good to hint that the intrinsic scatter in the relations is less than the adopted 0.14, in agreement with the discussion above. Indeed if the possible period dependence of the projection factor p discussed in section 4.2.1 applies, these two stars lie even more closely on a line with the Matsunaga et al. slope. They would then be 0.09 mag (V533 Cen) and 0.08 mag (SW Tau) brighter than

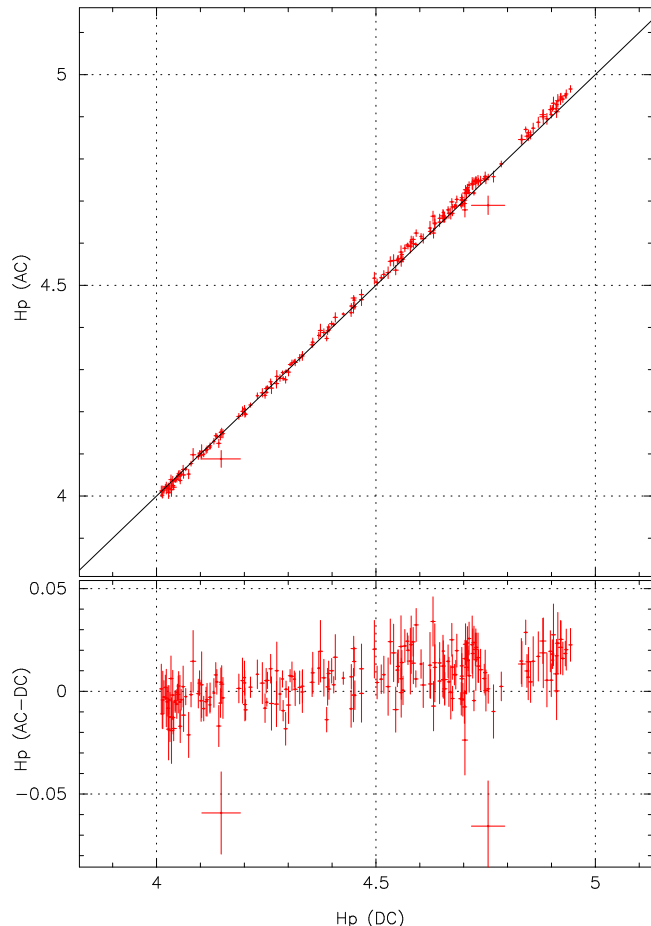


Figure 11. The relation between the Hipparcos AC and DC magnitudes for κ Pav. The increasing discrepancy between the AC and DC magnitudes towards fainter magnitudes is an indication for the presence of a close companion that becomes more visible as κ Pav becomes fainter.

Table 6. Differences from Infrared PL relations

Star	ΔM_K	σ_1	σ_2
(a)			
RR Lyrae	-0.24	0.11	0.17
VY Pyx	+0.30	0.19	0.24
κ Pav	+0.04	0.26	0.30
(b)			
κ Pav	-0.46	0.07	0.16
V533 Cen	-0.05	0.08	0.16
SW Tau	+0.02	0.08	0.16

(a) Results using trigonometrical parallaxes.

(b) Results using pulsational parallaxes.

that predicted using a zero-point based on an LMC modulus of 18.39. Both SW Tau and V533 Cen are carbon-rich stars of near solar metallicity. SW Tau has $[Fe/H] = +0.22$ (Maas et al. 2007) and V533 Cen has $[Fe/H] = +0.04$ (Wallerstein & Gonzales 1996). The light-curve classification scheme proposed by Diethelm (1990 and other papers referenced there) indicates that, as one would expect, these two stars are disc

objects. On the other hand the short-period globular-cluster stars ($P < 5$ days) in Matsunaga et al. (2006) are all of low metallicity ($[\text{Fe}/\text{H}]$ in the range -1.15 to -1.94). Thus within the uncertainties, the $\text{PL}(K_s)$ relation for CephIIs is insensitive to population differences (metallicity, mass) at least at the short period end.

The pulsation parallax of κ Pav leads to an infrared absolute magnitude that differs significantly from the PL relations derived from the globular clusters and with an LMC modulus of 18.39. Since the formal uncertainty of the pulsation-based absolute magnitude is 0.07 mag the deviation is 6.5σ and even taking into account the upper limit on the intrinsic scatter in the $\text{PL}(K_s)$ relation there is nearly a three sigma deviation. Evidently if this result is accepted then some CephIIs in the field can deviate significantly from the $\text{PL}(K_s)$ based on globular cluster variables. Since the metallicity of κ Pav is near solar and the results of Matsunaga et al. depend on metal-poor objects, a (large) metallicity effect might be the cause. As there is little metallicity dependence among the metal-poor objects (see section 2.2) this would imply a very non-linear dependence on metallicity. An age/mass difference would be another possible cause (possibly operating more strongly among the longer period CephIIs like κ Pav than among the shorter period one).

If one adopts the results from the three pulsation parallaxes, an LMC modulus of 18.55 ± 0.15 is implied, neglecting any metallicity effect on CephII luminosities. This agrees with the RR Lyrae result given above which implies a modulus of 18.55 ± 0.12 . Neither of these values are significantly different from the classical Cepheid result (18.39 ± 0.05). However, the smaller distance for κ Pav indicated by the revised Hipparcos result and the discussion of section 5.1, suggests that, for the present, the results for this star should be viewed with some caution. Additional pulsation parallaxes of CephIIs with periods near 10 days and/or an improved trigonometrical parallax of κ Pav would no doubt throw more light on this problem.

5.3 A Type II Cepheid distance scale

In section 5.2 we compared the Galactic Cepheid distance scale with that implied by the Classical Cepheid scale (with metallicity corrections). In this section we derive distance moduli for the LMC and for the Galactic Centre, based directly on CephIIs. The two stars V553 Cen and SW Tau give a mean zero-point, c in eq. 4 of -1.01 ± 0.06 where the standard error comes from the standard errors of the two stars. If the pulsation parallax result for κ Pav is included the zero-point becomes $c = -1.16 \pm 0.15$ where the standard error is based on the intergrement of the three stars.

Matsunaga et al. (2006) list 2MASS, single-epoch, J, H, K_s photometry of LMC CephII stars with known periods from Alcock et al. (1998). There are 21 such stars with log $P < 1.50$. Longer period stars are not considered here as they may be RV Tau stars. After correcting by $A_{K_s} = 0.02$ mag for absorption these data were fitted to a line of the slope derived by Matsunaga et al. (eq.4) viz:

$$K_s^o = -2.41 \log P + \gamma. \quad (8)$$

We then find $\gamma = 17.31 \pm 0.08$ or if one somewhat discrepant star is omitted $\gamma = 17.36 \pm 0.07$. With the values of

c in the previous paragraph these lead to the following estimates of the LMC modulus: for 21 LMC stars, a modulus of 18.31 ± 0.10 from V553 Cen and SW Tau, or 18.47 ± 0.17 if we included κ Pav. Leaving out the discrepant LMC star we obtain for the two or three star solutions, 18.37 ± 0.09 and 18.52 ± 0.16 . Pending further work on κ Pav, the best value is probably 18.37 ± 0.09 but none of the values deviate significantly from the Classical Cepheid value 18.39 ± 0.05 .

Groenewegen et al. (2008) have recently estimated mean K_s values and periods for 39 CephIIs in the Galactic Bulge. After correction for absorption they fit their data to an equation equivalent to eq. 8 above. Their result gives, $\gamma = 13.404 \pm 0.013$. This together with the results for V553 Cen and SW Tau leads to a modulus of the Galactic Centre of 14.42 ± 0.06 and to a Galactic Centre distance of $R_0 = 7.64 \pm 0.21$ kpc. If we include κ Pav we obtain 14.56 ± 0.15 and $R_0 = 8.18 \pm 0.56$ kpc. The first value, which at present should probably be considered the preferred one, is close to that obtained by Eisenhauser et al. (2005) from the motion of a star close to the central black-hole. With the suggested relativistic correction of Zucker et al. (2006) this is, $R_0 = 7.73 \pm 0.32$ kpc. The value with κ Pav included does not differ significantly from this latter result.

5.4 Optical period-luminosity relations

The relations derived for CephIIs in the globular clusters NGC 6441 and NGC 6388 (eqs. 5,6,7 above) at optical wavelengths, are quite narrow (see Pritzl et al. 2003, fig. 8). On the other hand, plots of period-luminosity diagrams in B, V or I for all known data for globular clusters and the LMC (e.g. Pritzl et al. fig. 9) show very considerable scatter. Pritzl et al. suggested that at least part of this scatter might be due to poor photometry. This left open the question as to whether general PL relations are as narrow as they found for their two clusters. In Table 7 are the deviations of our programme stars from eqs. 5,6,7. Table 7a gives the results from the trigonometrical parallaxes and Table 7b those from the pulsation parallaxes. In the case of the trigonometrical result for κ Pav the deviations are within the expected uncertainty (0.26) whereas they are large for the pulsation parallax result which has a small internal error (0.07). As discussed in section 5.1 we prefer to leave a solution of this matter to further work. The pulsation parallax results for V553 Cen and SW Tau are of special interest since their formal uncertainties are small (0.08). These two stars have deviations of opposite signs both from the optical and infrared relations (Tables 7 and 6). The difference between these two deviations thus gives an estimate of the lower limit of the PL width at different wavelengths, independent of PL zero-point considerations. These differences are: 0.77 mag at B , 0.51 at V , 0.20 at I and 0.07 at K_s . The results for VY Pyx, though of lower accuracy agree with these results. This increase in the dispersion with decreasing wavelength is, as in the case of classical Cepheids, naturally explained by the existence of a finite instability strip.

The optical differences just quoted are significantly greater than the rms scatter about the PL relations in NGC 6441 and NGC 6388 given by Pritzl et al. (2003) which are 0.10, 0.07 and 0.06 in B, V, I . The possibility that the greater optical differences estimated from V553 Cen and SW Tau are due to the adoption of incorrect reddening cor-

Table 7. Deviation from optical relations.

star	eq. 6	eq. 5	eq. 7
	ΔM_B	ΔM_V	ΔM_I
(a)			
VY Pyx	+0.89	+0.64	
κ Pav	-0.27	-0.34	-0.10
(b)			
κ Pav	-0.77	-0.77	-0.60
V553 Cen	+0.56	+0.26	+0.09
SW Tau	-0.21	-0.25	-0.11

(a) Results using trigonometrical parallaxes.

(b) Results using pulsational parallaxes.

rections for these two stars seems unlikely. The lower scatter in the case of the clusters is thus probably due to the smaller range in the masses of the cluster variables compared with the field.

The evolutionary state of the metal-rich, short-period, CephIIs in the field has long constituted something of a puzzle (see for instance section 4 of Wallerstein 2002). As briefly summarized in section 1, the short period CephII stars are thought to be moving through an instability strip as they evolve from the blue HB towards the AGB. Old metal-rich globular clusters have, in general, only stubby red HB and it is not clear how stars of the ages and metallicities of these systems could evolve into the CephII instability strip. NGC 6441 and NGC 6388 are well known as metal-rich systems which do have extended blue HBs. There has been much discussion in the literature on the cause of this anomaly in these and similar clusters. One possibility is that the effect is due to enhanced helium abundance derived from earlier generations of stars in the clusters (see for instance; Lee et al. 2007, Caloi & D’Antona 2006, based on earlier work by Rood 1973 and others). This seems unlikely to apply to field, short-period, metal-rich, CephIIs. Thus either an alternative explanation has to be found which will apply to both the field and cluster stars, or, some other means will need to be found to move the field stars into the instability strip.

6 CONCLUSIONS

Parallaxes of RR Lyrae variables from the revised Hipparcos catalogue (van Leeuwen 2007) have been investigated. The parallax of RR Lyrae itself obtained by combining the revised Hipparcos value with an HST determination (Benedict et al. 2002) outweighs that of all other members of the class. It yields $M_{K_s} = -0.64 \pm 0.11$ which is 0.16 ± 0.12 mag brighter than that implied by observations of RR Lyrae variables in the LMC with a modulus of 18.39 ± 0.05 derived from classical Cepheids (Benedict et al. 2007, van Leeuwen et al. 2007). For 142 Hipparcos RR Lyrae variables mean J, H, K_s based on phased-corrected 2MASS values are given. These should be useful when discussing the proper motions and radial velocities of the stars. Revised Hipparcos parallaxes for the CephIIs κ Pav and VY Pyx are given, and pulsation parallaxes for κ Pav, V553 Cen and SW Tau de-

rived. Extensive new J, H, K photometry of some of these stars and of some classical Cepheids is tabulated. The latter data are used to establish 1.23 as the most appropriate “ p -factor” to use in the pulsational analysis of Cepheids. The short-period, metal- and carbon-rich, disc population CephIIs V553 Cen and SW Tau have pulsation-based absolute magnitudes of high internal accuracy (± 0.08 mag). They fit closely (mean deviation 0.02 mag) the $PL(K_s)$ relation derived by Matsunaga et al. (2006) from CephIIs in globular clusters and with a zero-point fixed by adopting an LMC modulus of 18.39. The Hipparcos parallax of the short period star VY Pyx, although it has higher uncertainty, agrees with this result. This suggests that at least at short periods the CephIIs in the Galactic disc and in Globular clusters fit the same $PL(K_s)$ relation rather closely. The scatter of V553 Cen and SW Tau about the optical PL relations derived by Pritzl et al. (2003) for the globular clusters NGC 6388 and NGC 6441 is much greater than that about the Matsunaga $PL(K_s)$ relation, showing the expected increase in PL widths with decreasing wavelength. This scatter about the optical relations is also much greater than that of the CephIIs in NGC 6388/6441 themselves. Since the values of $[Fe/H]$ are very similar for V553 Cen and SW Tau this is unlikely to be due to a metallicity effect. It presumably indicates a larger spread in masses for the short period CephIIs in the general field than for those in the clusters.

The Hipparcos and pulsation parallaxes of the long-period star κ Pav differ by about 2σ . If the pulsation parallax is adopted, the value of M_{K_s} (which is of high internal accuracy, $\sigma = 0.07$ mag) is more than 6σ from the Matsunaga relation with a zero-point fixed by an LMC modulus of 18.39 and would suggest a significant mass or metallicity effect at about this period (~ 10 days). There are indications that this star may have a close companion. In view of this, further work on the star and of others of similar period is desirable before discussing in detail the implications for long-period CephIIs.

The results for V553 Cen and SW Tau together with published data on CephIIs in the LMC and the Galactic Bulge lead to an LMC modulus of 18.37 ± 0.09 and to a distance to the Galactic centre of $R_0 = 7.64 \pm 0.21$ kpc. Including the data for κ Pav would increase these estimates by ~ 0.15 mag.

ACKNOWLEDGMENTS

This publication makes use of data products from the Two Micron All Sky Survey, which is a joint product of the University of Massachusetts and the Infrared Processing and Analysis Center/California Institute of Technology, funded by the National Aeronautics and Space Administration and the National Science Foundation. We are grateful to the referee for their comments.

REFERENCES

- Alcock C. et al. 1998, AJ, 115, 1921
- Arellano Ferro A., Rojo Arellano E., Gonzalez-Bedolla S., Rosenzweig, P., 1998, ApJS, 117, 167
- Balog Z., Vinko J., Kaszas, G., 1997, AJ, 113, 1833
- Balona L.A., 1977, 231

- Barnes, T.G., Moffett, T.J., Freuh, M.L., 1992, *PASP*, 104, 514
- Barnes T.G., Fernley J.A., Freuh M.L., Navas J.G., Moffett I.J., Skillen I., 1997, *PASP*, 109, 645
- Barnes T.G., Moffett T.J., Slovak M.H. 1987, *ApJS*, 65, 307
- Benedict G.F. et al., 2002a, *AJ*, 123, 473
- Benedict G.F., McArthur B.E., Fredrick L.W., Harrison T.E., Slesnick C. L., Rhee J., Patterson R.J., Skrutskie M.F., Franz O.G., Wasserman L.H., Jefferys W.H., Nelan E., van Altena W., Shelus P.J., Hemenway P.D., Duncombe R.L., Story D., Whipple A.L., Bradley A.J., 2002b, *AJ*, 124, 1695
- Benedict G.F., McArthur B.E., Feast M.W., Barnes T.G., Harrison T.E., Patterson R.J., Menzies J.W., Bean J.L., Freedman W.L., 2007, *AJ*, 133, 1810
- Berdnikov L.N., Turner D.G., 1995, *PAZh*, 21, 803
- Berdnikov L.N., 1997, *CDS Vizier Catalogue II/217*
- Berdnikov L.N., Turner D.G., 2001, *ApJS*, 137, 209
- Bersier D., 2002, *ApJS*, 140, 465
- Bersier D., Burki G., Mayor M., Duquenois A., 1994, *A&AS*, 108, 25
- Butler R.P., 1993, *ApJ*, 415, 323
- Caloi V., D'Antona F., 2007, *A&A*, 463, 949
- Carpenter J.M., 2001, *AJ*, 121, 2851
- Carter B.S., 1990, *MN*, 242, 1
- Catalan M., Cortés C., 2008, arXiv:0802.2063
- Cester, B., Todoran, I., 1976, *MemSAI*, 47, 217
- Clementini G. Ripepi V., Bragaglia A., Martinez Fiorenzano A.F., Held E.V., Gratton R.G., 2005, *MNRAS*, 363, 734
- Cousins A.W.J., Lagerweij H.C., 1971, *MNASSA*, 30, 13
- Cutri, R., Skrutskie, M., Van Dyk, S., Beichmann, C., Carpenter, J., Chester, T. et al., 2003, University of Massachusetts and Infrared Processing and Analysis Center (IPAC/California Institute of Technology).
- Elias J.H., Frogel J.A., Matthews K., Neugebauer G., 1982, *AJ*, 87, 1029 (Erratum 1982, *AJ*, 87, 1893)
- Elias J.H., Frogel J.A., Hyland A.R., Jones T.J., 1983, *AJ*, 88, 1027
- Dean J.F., 1977, *MNASSA*, 36, 3
- Dean J.F., 1981, *SAAO Circulars*, 6, 10
- Dean J.F., Cousins A.W.J., Bywater R.A., Warren P.R., 1977, *MmRAS*, 83, 69
- Diethelm R., 1986, *A&AS*, 64, 261
- Diethelm R., 1990, *A&A*, 239, 186
- Drimmel R., Cabrera-Lavers A., López-Corredoira M, 2003, *A&A* 409, 205
- Duncan J.C., 1932, *PASP*, 44, 324
- Eggen O.J., 1985, *AJ*, 90, 1297
- Feast M.W., 1967, *MN*, 136, 141
- Eisenhauer F. et al., 2005, *ApJ*, 628, 246
- ESA, 1997, *The Hipparcos catalogue ESA SP-1200*
- Feast M.W., 2002, *MNRAS*, 337, 1035
- Fernie J.D., 1995, *AJ*, 110, 2361
- Fernley J.A., Skillen I., Jameson R.F., Longmore A.J., 1990, *MNRAS*, 242, 685
- Fernley, J.A., Skillen, I., Burki G., 1993, *A&ASup*, 97, 815
- Fernley J.A., Barnes T.G., Skillen I., Hawley S.L., Evans D.W., Solano E., Garrido R., 1998, *A&A*, 330, 515
- Fouqué P., Arriagada P., Storm J., Barnes T.G., Nardetto N., Merand A., Kervella P., Gieren W., Bersier D., Benedict G.F., McArthur B.E., 2007, *A&A*, 476, 73
- Fouqué P., Arriagada P., Storm J., Barnes T.G., Nardetto N., Méand A., Kervella P., Gieren W., Bersier D., Benedict G.F., McArthur B.E., 2007, *A&A*, 476, 73
- Gieren W.P., Fouqué P., Gomez M.I., 1997, *ApJ*, 488, 74
- Gieren W.P., Fouqué P., Gomez M.I., 1998, *ApJ*, 496, 17
- Gingold R.A., 1976, *ApJ*, 204, 116
- Gingold R.A., 1985, *Mem.Soc.Ast.It.* 56, 169
- Gorynya N.A., Samus N.N., Sachkov M.E., Rastorguev A.S., Glushkova E.V., Antipin S.V., 1998, *Ast. Letters*, 24, 815
- Gratton R.G., Bragaglia A., Carretta E., Clementini G., Desidera S., Grundahl F., Lucatello S., 2003, *A&A*, 408, 529
- Gratton R.G., Bragaglia A., Clementini G., Carretta E., Di Fabrizio L., Maio M., Taribello E., 2004, *A&A*, 421, 937
- Gray R.O., Olsen E.H., 1991, *A&AS*, 87, 541
- Groenewegen M.A.T., 2007, *A&A*, 474, 975
- Groenewegen M.A.T., Udalski A., Bono G., 2008, arXiv:0801.2652
- Hindsley R.B., Bell R.A., 1990, *ApJ*, 348, 673
- Janot-Pacheco E., 1976, *A&ASup*, 25, 159
- Jones, R.V., Carney, B.W., Storm, J., Latham, D.W., 1992, *ApJ*, 386, 646
- Jones, R.V., Carney, B.W., Fulbright, J.P., 1996, *PASP*, 108, 877
- Kiss L.L., 1998, *MN*, 297, 825
- Kiss L.L., Csák B., Thomson J.R., Szatmáry K., 1999, *IBVS No.* 4660
- Laney C.D., 1995, in *Astrophysical Applications of Stellar Pulsation*, ASP Conf. Series, Vol. 83, 367
- Laney C.D., Caldwell J.A.R., 2007, *MN*, 377, 147
- Laney C.D., Stobie R.S., 1992 *A&ASup*, 93, 93
- Laney C.D., Stobie R.S., 1993, *MN*, 263, 921
- Laney C.D., Stobie R.S., 1995, *MN*, 274, 337 (=LS95)
- Lee Y-W., Gim H.B., Casetti-Dinescu D.I., 2007, arXiv:0704.0486
- Lloyd Evans T., 1968, *MN*, 141, 109
- Lloyd Evans T., 1980, *SAAO Circulars*, 1, No.5, 257
- Lloyd Evans T., Wisse P.N.J., Wisse M., 1972, *MN*, 159, 67
- Longmore A.J., Fernley J.A., Jameson R.F., 1986, *MNRAS*, 220, 279
- Luck R.E., Bond H.E., 1989, *ApJ*, 342, 476
- Maas T., Giridhar S., Lambert D.L., 2007, *ApJ*, 666, 378
- Macri L.M., Stanek K.Z., Bersier D., Greenhill L.J., Reid M.J., 2006, *ApJ*, 652, 1133
- Maintz, G., 2005, *A&A* 442, 381
- Mathias P., Gillet D., Fokin A.B., Nardetto N., Kervella P., Mourard D., 2006, *A&A*, 457, 579
- Matsunaga N., Fukushi H., Nakada Y., Tanabe T., Feast M.W., Menzies J.W., Ita Y., Nishiyama S., Baba D., Takahiro T., Nakaya H., Takahiro K., Ishihara A., Kato D., 2006, *MN*, 370, 1979
- Merand A., Kervella P., Coude du Foresto V., Ridgway S.T., Aufdenberg J.P., ten Brummelaar T.A., Berger D.H., Sturmann J., Sturmann L., Turner N.H., McAlister H.A., 2005, *A&A*, 438, L9
- Moffett T.J., Barnes T.G., 1984, *ApJS*, 55, 389
- Moore J.H., 1909, *Lick Obs. Bull.*, 5, 111
- Nardetto N., Mourard D., Mathias P., Fokin A., Gillet D., 2007, *A&A*, 471, 661
- Nikolov, N., Buchantsova, N., Frolov, M., 1984 (Mean Light curves of 210 Field RR Lyrae type Stars) Published by the Dept. of Astronomy, Faculty of Physics Astronomical Council of the USSR Academy of Sciences for Department of Astronomy, University of Sofia.
- Pel J.W., 1976, *A&ASup*, 24, 413
- Pojmanski, G., 2002, *Acta Astronomica*, 52, 397 (ASAS Catalogue)
- Popowski P., Gould A., 1998, *AJ*, 506, 259
- Pritzl B.J., Smith H.A., Stetson P.B., Catelan M., Sweigart A.V., Layden A.C., Rich R.M., 2003, *AJ*, 126, 1381
- Rood R.T., 1973, *ApJ*, 184, 815
- Salaris M., Held E.V., Ortolani S., Gullieuszik M., Momany Y., 2007, *A&A*, 476, 243
- Sandage A., Tammann G.A., 2006, *ARA&A*, 44, 93
- Sanwal N.B., Sarma M.B.K., 1991, *J.Astroph.Ast.*, 12, 119
- Sasselov D.D., Lester J.B., 1990, *ApJ*, 362, 333
- Schmidt E.G., 1991, *AJ*, 102, 1766
- Shobbrook R.R., 1992, *MN*, 255, 486
- Sollima A., Cacciari C., Valenti E., 2006, *MNRAS*, 372, 1675
- Sollimia A., Cacciari C., Arkharov A.A., Larionov V.M.,

- Gorshanov D.L., Efimova N.V., Piersimoni A., 2007, arXiv:0712.0578
- Stibbs D.W.N., 1955, MN, 115, 363
- Stobie R.S., Balona L.A., 1979, MN, 189, 641
- Szabados L. 1981, Comm. Konkoly Obs., No.77, 1
- Szabados L., 1990, MN, 242, 285
- Taylor M.M., Booth A.J., 1998, MN, 298, 594
- Taylor M.M., Albrow M.D., Booth A.J., Cottrell P.L., 1997, MN, 292, 662
- van Leeuwen F., Feast M.W., Whitelock P.A., Laney C.D., 2007, MNRAS, 379, 723
- van Leeuwen F., 2007a, Hipparcos, the New Reductions of the Raw Data. Springer, Berlin, in press
- van Leeuwen F., 2007b, A&A, 474, 653
- Wallerstein G., Gonzalez G., 1996, MN, 282, 1236
- Wallerstein G., Jacobsen T.S., Cottrell P.L., Clark M., Albrow M., 1992, MN, 259, 474
- Wallerstein G., 2002, PASP, 114, 689
- Whitelock P.A., Feast M.W., van Leeuwen F., 2008, MNRAS, submitted
- Wils, P., Lloyd, C., Bernhardt, K., 2006, MNRAS, 368, 1757
- Wilson T.D., Carter M.W., Barnes T.G., Van Citters G.W., Moffett T.J., 1989, ApJS, 69, 951
- Wisse P.N.J., Wisse M., 1970, MNSSA, 29, 151
- Zucker S., Alexander T., Gillessen S., Eisenhauer F., Genzel R., 2006, ApJ, 639, L21

APPENDIX A: INFRARED PHOTOMETRY

Previously unpublished *JHK* observations for classical Cepheids ζ Gem and X Sgr, and for the CephIIs, V553 Cen, κ Pav and SW Tau are given in Table A1. These data were obtained by CDL with the IRP Mk II photometer and 0.75m telescope at the Sutherland observing station of the South African Astronomical Observatory (SAAO), exactly as for the classical Cepheid data given in Laney & Stobie (1992). This single-channel device was used with a 36 arcsec aperture and a chopping distance of 3 arcmin, and is particularly suited to bright objects. The data are on the SAAO standard system (Carter 1990), which was established with the same telescope, photometer and filter set. Accuracy is typically 0.005-0.008 mag for bright stars, including standardization. Similar data for ι Car and β Dor has been taken from Laney & Stobie (1992), while IR data for δ Cep on the CIT system was taken from Barnes et al. (1997) and transformed to the Carter system by the formulae given in Laney & Stobie (1993). For convenience, these data are given in Table A1 as well, with the phases and $V - K$ values calculated for the radius solutions used here.

Table A1: Data for B-W solutions

δ Cep						
JD	Phase	K	H	J	$V - K$	L
2448429.980	0.2532	2.250	2.310	2.671	1.621	
2448430.953	0.4346	2.275	2.346	2.761	1.817	
2448431.985	0.6269	2.372	2.442	2.885	1.913	
2448433.888	0.9815	2.301	2.349	2.612	1.219	
2448434.969	0.1829	2.256	2.310	2.646	1.510	
2448435.947	0.3652	2.273	2.338	2.732	1.747	
2448436.958	0.5536	2.320	2.388	2.812	1.888	
2448437.941	0.7368	2.444	2.521	2.939	1.900	
2448438.912	0.9177	2.385	2.433	2.732	1.364	
2448804.979	0.1343	2.254	2.309	2.632	1.439	
2448805.964	0.3178	2.251	2.325	2.705	1.706	
2448807.942	0.6864	2.411	2.484	2.917	1.921	
2448808.930	0.8706	2.429	2.491	2.833	1.589	
2448864.824	0.2864	2.231	2.296	2.668	1.685	
2448865.799	0.4681	2.286	2.343	2.763	1.834	
2448867.941	0.8673	2.434	2.494	2.849	1.601	
2448870.747	0.3902	2.265	2.312	2.728	1.784	
2448871.829	0.5918	2.349	2.419	2.847	1.901	
2448872.920	0.7951	2.458	2.528	2.939	1.837	
2448873.680	0.9367	2.343	2.393	2.669	1.309	
2448873.976	0.9919	2.284	2.332	2.586	1.227	
2449170.983	0.3391	2.250	2.309	2.705	1.736	
2449172.912	0.6986	2.421	2.493	2.926	1.917	
2449173.945	0.8911	2.401	2.462	2.783	1.500	
2449174.952	0.0787	2.264	2.315	2.603	1.347	
2449175.900	0.2554	2.250	2.311	2.673	1.624	
2449176.984	0.4574	2.287	2.351	2.760	1.824	
X Sgr						
JD	Phase	K	H	J	$V - K$	L
2448846.455	0.7242	2.627	2.745	3.189	2.229	
2448849.447	0.1509	2.451	2.541	2.918	1.928	
2448850.461	0.2955	2.458	2.558	2.968	2.064	
2448851.393	0.4284	2.487	2.591	3.025	2.188	
2448852.429	0.5761	2.549	2.655	3.114	2.279	
2449263.318	0.1685	2.444	2.541	2.923	1.956	
2449291.232	0.1490	2.444	2.545	2.907	1.933	
2449292.231	0.2914	2.452	2.547	2.961	2.068	
2449534.463	0.8335	2.627	2.724	3.119	2.004	
2449535.472	0.9773	2.509	2.603	2.927	1.756	
2449537.453	0.2598	2.438	2.542	2.930	2.064	
2449538.451	0.4021	2.473	2.572	2.996	2.160	
2449598.329	0.9407	2.539	2.623	2.951	1.776	
2449601.312	0.3661	2.469	2.559	2.982	2.111	
2449859.677	0.2086	2.452	2.538	2.925	2.000	
2449878.570	0.9028	2.588	2.671	3.015	1.823	
2449889.482	0.4588	2.496	2.600	3.048	2.227	
2449890.517	0.6064	2.561	2.667	3.128	2.277	
2449941.461	0.8709	2.597	2.692	3.060	1.913	
2449942.472	0.0151	2.478	2.571	2.900	1.782	
2450142.667	0.5627	2.549	2.656	3.102	2.274	
2450157.671	0.7023	2.618	2.717	3.165	2.246	
2450160.679	0.1312	2.453	2.545	2.906	1.904	
2450682.301	0.5139	2.510	2.612	3.060	2.280	
2450683.405	0.6714	2.595	2.689	3.148	2.265	
2450685.354	0.9493	2.516	2.610	2.936	1.783	
2450912.682	0.3660	2.456	2.554	2.964	2.124	
2450219.546	0.5256	2.533	2.630	3.088	2.268	
2450221.553	0.8118	2.631	2.731	3.145	2.066	
2450240.470	0.5093	2.505	2.622	3.069	2.282	
2450244.557	0.0921	2.468	2.554	2.911	1.852	
2449445.690	0.1745	2.444	2.542	2.906	1.965	
2449590.389	0.8084	2.632	2.727	3.159	2.074	

2449620.321	0.0767	2.476	2.558	2.910	1.830	
2450262.466	0.6459	2.593	2.694	3.145	2.258	
2450262.509	0.6520	2.578	2.692	3.140	2.275	
β Dor						
Period 9.842578 Epoch 2447913.2106						
JD	Phase	<i>K</i>	<i>H</i>	<i>J</i>	<i>V - K</i>	<i>L</i>
2447516.626	0.7072	2.073	2.131	2.537	1.742	
2447517.537	0.7998	2.044	2.107	2.466	1.640	
2447518.630	0.9108	1.987	2.041	2.401	1.627	
2447520.269	0.0774	1.900	1.968	2.358	1.643	
2447521.605	0.2131	1.856	1.922	2.348	1.825	
2447522.287	0.2824	1.877	1.945	2.381	1.911	
2447524.511	0.5084	1.994	2.070	2.531	2.087	
2447525.362	0.5948	2.054	2.134	2.579	1.981	
2447526.346	0.6948	2.057	2.136	2.531	1.772	
2447528.533	0.9170	1.983	2.049	2.419	1.622	
2447534.370	0.5100	1.995	2.076	2.562	2.086	1.894
2447567.352	0.8610	2.010	2.076	2.448	1.637	
2447570.367	0.1673	1.869	1.929	2.323	1.760	
2447604.320	0.6169	2.055	2.136	2.560	1.948	
2447607.269	0.9165	1.982	2.044	2.415	1.623	
2447642.251	0.4707	1.979	2.050	2.528	2.072	
2447643.229	0.5700	2.045	2.124	2.589	2.008	
2447644.221	0.6708	2.058	2.132	2.531	1.811	
2447645.203	0.7706	2.051	2.107	2.488	1.680	
2447646.194	0.8713	1.998	2.070	2.450	1.646	
2447647.249	0.9785	1.918	1.988	2.330	1.535	
2447660.204	0.2947	1.883	1.948	2.380	1.924	1.790
2447670.194	0.3097	1.892	1.955	2.408	1.935	
2447675.187	0.8169	2.023	2.088	2.459	1.643	
2447676.193	0.9192	1.982	2.048	2.422	1.619	
2447713.698	0.7296	2.054	2.137	2.514	1.739	
2447714.684	0.8298	2.009	2.085	2.455	1.649	
2447715.727	0.9358	1.972	2.037	2.371	1.592	
2447716.716	0.0363	1.902	1.980	2.316	1.577	
2447719.719	0.3414	1.891	1.972	2.420	1.982	
2447727.698	0.1520	1.875	1.940	2.330	1.731	
2447731.687	0.5573	2.041	2.113	2.589	2.019	
2447742.689	0.6751	2.062	2.135	2.538	1.798	
2447744.673	0.8767	2.003	2.067	2.445	1.639	1.897
2447759.672	0.4006	1.923	2.001	2.473	2.047	1.823
2447769.689	0.4183	1.941	2.009	2.494	2.048	
2447803.622	0.8659	2.001	2.071	2.436	1.645	
2447811.633	0.6798	2.058	2.134	2.533	1.793	
2447815.547	0.0774	1.904	1.962	2.343	1.639	1.800
2447816.620	0.1865	1.868	1.939	2.347	1.785	1.770
2447821.586	0.6910	2.061	2.129	2.528	1.772	1.954
2447823.528	0.8883	1.996	2.057	2.443	1.641	1.903
ζ Gem						
Period 10.14992 Epoch 2450180.19683						
JD	Phase	<i>K</i>	<i>H</i>	<i>J</i>	<i>V - K</i>	<i>L</i>
2448317.332	0.4651	2.142	2.228	2.697	2.029	
2448318.339	0.5643	2.205	2.278	2.730	1.944	
2448320.323	0.7598	2.200	2.266	2.655	1.689	
2449789.295	0.4872	2.157	2.238	2.703	2.022	
2449790.260	0.5823	2.209	2.292	2.724	1.919	
2450079.492	0.0783	2.076	2.149	2.523	1.653	
2450082.476	0.3723	2.103	2.185	2.648	1.982	
2450147.267	0.7557	2.192	2.268	2.656	1.701	
2450149.304	0.9563	2.118	2.171	2.541	1.589	
2450150.279	0.0524	2.085	2.140	2.522	1.626	
2450151.269	0.1499	2.057	2.121	2.528	1.742	
2450152.253	0.2469	2.054	2.120	2.551	1.867	
2450155.274	0.5445	2.192	2.278	2.732	1.974	
2450156.300	0.6456	2.220	2.287	2.697	1.815	
2450157.270	0.7412	2.207	2.277	2.659	1.700	
2450158.257	0.8384	2.163	2.225	2.597	1.651	
2450159.274	0.9386	2.127	2.183	2.551	1.591	

2450160.283	0.0380	2.080	2.142	2.509	1.623
2450161.268	0.1351	2.049	2.115	2.511	1.734
2450471.427	0.6929	2.208	2.282	2.680	1.757
2450472.418	0.7905	2.192	2.256	2.635	1.668
2450473.400	0.8872	2.140	2.212	2.573	1.624
2450474.396	0.9854	2.096	2.154	2.517	1.600
2450475.397	0.0840	2.058	2.144	2.509	1.675
2450476.386	0.1814	2.050	2.121	2.532	1.787
2450824.411	0.4699	2.165	2.236	2.705	2.009
2450827.407	0.7651	2.192	2.260	2.637	1.692
2450886.262	0.5636	2.196	2.284	2.722	1.953
2451155.527	0.0924	2.065	2.127	2.522	1.676
2451177.479	0.2552	2.072	2.141	2.584	1.860

ℓ Car

Period 35.543270 Epoch 2446104.2086

JD	Phase	<i>K</i>	<i>H</i>	<i>J</i>	<i>V</i> - <i>K</i>	<i>L</i>
2446575.359	0.2557	0.973	1.088	1.656	2.684	
2446576.304	0.2823	0.971	1.088	1.659	2.719	
2446597.218	0.8707	1.286	1.383	1.904	2.467	1.119
2446601.246	0.9840	1.129	1.242	1.694	2.225	
2446603.261	0.0407	1.069	1.185	1.662	2.300	
2446607.256	0.1531	1.012	1.118	1.648	2.509	
2446609.251	0.2092	0.975	1.081	1.635	2.624	
2446610.264	0.2377	0.990	1.097	1.642	2.645	
2446611.230	0.2649	0.978	1.099	1.662	2.690	
2446740.634	0.9057	1.220	1.341	1.812	2.345	
2446741.617	0.9333	1.183	1.289	1.755	2.265	
2446758.567	0.4102	1.007	1.133	1.736	2.867	0.843
2446782.560	0.0852	1.033	1.157	1.652	2.387	0.924
2446803.518	0.6749	1.150	1.280	1.879	2.917	0.980
2446834.413	0.5441	1.077	1.202	1.828	2.954	0.903
2446862.546	0.3356	0.985	1.099	1.682	2.787	
2446863.548	0.3638	0.983	1.108	1.702	2.834	
2446880.261	0.8340	1.274	1.396	1.938	2.651	
2446881.505	0.8690	1.275	1.398	1.899	2.487	
2446886.494	0.0094	1.098	1.210	1.664	2.253	
2446898.356	0.3431	0.978	1.086	1.675	2.806	0.817
2446899.341	0.3708	0.974	1.099	1.698	2.854	0.826
2446914.315	0.7921	1.267	1.394	1.964	2.756	1.126
2446915.396	0.8225	1.274	1.403	1.966	2.689	1.129
2446967.254	0.2815	0.946	1.071	1.637	2.743	0.830
2446972.286	0.4231	1.010	1.129	1.726	2.876	
2446978.260	0.5912	1.110	1.243	1.863	2.944	
2446981.247	0.6752	1.192	1.318	1.907	2.874	
2446982.239	0.7031	1.207	1.334	1.932	2.856	
2446983.240	0.7313	1.229	1.352	1.936	2.826	
2446985.207	0.7866	1.282	1.398	1.961	2.748	1.131

κ Pav

Period 9.0814 Epoch 2446684.0691

JD	Phase	<i>K</i>	<i>H</i>	<i>J</i>	<i>V</i> - <i>K</i>	<i>L</i>
2445928.495	0.7998	3.039	3.102	3.396	1.399	
2445929.486	0.9089	2.816	2.886	3.149	1.177	2.778
2445953.440	0.5466	2.861	2.945	3.355	1.896	
2446329.287	0.9331	2.799	2.856	3.105	1.154	
2446345.338	0.7006	3.041	3.110	3.465	1.594	
2446652.532	0.5273	2.859	2.934	3.354	1.893	
2446675.477	0.0539	2.673	2.733	3.013	1.275	
2446676.465	0.1627	2.646	2.715	3.045	1.518	
2446680.420	0.5982	2.924	3.003	3.405	1.821	
2446682.439	0.8205	3.012	3.067	3.353	1.330	
2446684.440	0.0408	2.680	2.750	3.033	1.252	
2446686.435	0.2605	2.654	2.732	3.111	1.740	
2446694.370	0.1343	2.639	2.706	3.026	1.463	2.584
2446703.267	0.1140	2.667	2.730	3.051	1.391	2.612
2446739.269	0.0783	2.656	2.725	3.001	1.331	
2446740.278	0.1895	2.645	2.716	3.058	1.580	
2446741.275	0.2992	2.669	2.745	3.136	1.801	
2446744.251	0.6269	2.952	3.019	3.420	1.763	2.868

2446748.245	0.0667	2.666	2.721	3.005	1.301
2446970.642	0.5560	2.875	2.953	3.366	1.883
2447029.481	0.0351	2.695	2.757	3.037	1.232
2447078.344	0.4157	2.737	2.818	3.238	1.942
2447646.640	0.9937	2.761	2.814	3.063	1.151
2447713.603	0.3673	2.729	2.802	3.202	1.863
2447715.598	0.5870	2.924	3.001	3.411	1.828

V553 Cen

Period 2.060464 Epoch 2448437.11540

JD	Phase	<i>K</i>	<i>H</i>	<i>J</i>	<i>V</i> - <i>K</i>	<i>L</i>
2446688.236	0.2206	6.755	6.851	7.180	1.631	
2446864.611	0.8203	6.974	7.053	7.357	1.452	
2446868.439	0.6781	6.992	7.083	7.408	1.595	
2446881.644	0.0868	6.789	6.860	7.153	1.470	
2446882.647	0.5736	6.973	7.073	7.431	1.725	
2446886.628	0.5057	6.919	7.013	7.386	1.815	
2446888.626	0.4754	6.900	6.991	7.367	1.814	
2446890.616	0.4412	6.874	6.973	7.350	1.801	
2446892.610	0.4089	6.852	6.939	7.309	1.782	
2446978.388	0.0394	6.809	6.887	7.171	1.422	
2446980.413	0.0222	6.819	6.893	7.186	1.407	
2446981.365	0.4842	6.905	6.998	7.377	1.817	
2446982.367	0.9705	6.862	6.942	7.223	1.365	
2447029.269	0.7333	7.004	7.094	7.414	1.562	
2447252.552	0.0987	6.784	6.858	7.155	1.485	
2447602.594	0.9838	6.853	6.929	7.215	1.372	
2447642.484	0.3435	6.810	6.906	7.260	1.742	
2447643.521	0.8468	6.957	7.034	7.328	1.409	
2447645.485	0.7999	6.990	7.064	7.365	1.481	
2447646.482	0.2838	6.791	6.871	7.220	1.676	
2447647.535	0.7949	6.989	7.067	7.371	1.493	
2447674.414	0.8400	6.929	7.021	7.323	1.452	
2447675.431	0.3336	6.795	6.881	7.239	1.743	
2447676.431	0.8189	6.976	7.058	7.351	1.453	
2447714.362	0.2278	6.775	6.861	7.196	1.619	
2447716.363	0.1990	6.766	6.849	7.180	1.597	
2447717.367	0.6863	7.005	7.083	7.411	1.579	
2447771.267	0.8454	6.973	7.029	7.332	1.396	

SW Tau

Period 1.583565d Epoch 2445013.2696

JD	Phase	<i>K</i>	<i>H</i>	<i>J</i>	<i>V</i> - <i>K</i>	<i>L</i>
2445950.650	0.9431	7.903	7.997	8.238	1.462	
2445953.656	0.8414	7.979	8.065	8.286	1.414	
2445954.643	0.4646	7.978	8.102	8.460	2.006	
2446023.497	0.9450	7.897	7.988	8.239	1.467	
2446024.407	0.5197	8.015	8.120	8.500	2.028	
2446069.412	0.9397	7.896	7.990	8.245	1.472	
2446073.364	0.4354	7.982	8.056	8.424	1.960	
2446075.340	0.6832	8.173	8.262	8.588	1.892	
2446326.631	0.3701	7.921	8.028	8.392	1.930	
2446326.654	0.3846	7.919	8.020	8.382	1.951	
2446334.623	0.4169	7.925	8.018	8.360	1.990	
2446335.654	0.0680	7.857	7.945	8.200	1.553	
2446338.664	0.9687	7.885	7.983	8.216	1.466	
2446345.613	0.3569	7.920	8.012	8.364	1.915	
2446363.537	0.6757	8.154	8.257	8.592	1.913	
2446427.296	0.9387	7.919	7.986	8.224	1.449	
2446664.636	0.8157	8.010	8.095	8.359	1.439	
2446676.646	0.3998	7.933	8.027	8.384	1.957	
2446677.645	0.0307	7.878	7.939	8.195	1.478	
2446682.640	0.1850	7.905	7.991	8.319	1.768	
2446686.649	0.7166	8.176	8.266	8.602	1.857	
2446693.609	0.1117	7.890	7.984	8.283	1.614	
2446702.618	0.8008	8.061	8.117	8.380	1.462	
2446739.479	0.0780	7.878	7.968	8.237	1.552	
2446740.568	0.7657	8.100	8.196	8.492	1.679	
2446741.614	0.4262	7.937	8.063	8.411	1.991	
2446744.481	0.2367	7.903	8.005	8.325	1.825	

2446745.469	0.8606	7.959	8.045	8.295	1.431
2446746.536	0.5344	8.044	8.155	8.501	2.010
2446747.484	0.1331	7.881	7.978	8.267	1.673
2446748.506	0.7784	8.086	8.154	8.421	1.594
2446780.359	0.8932	7.942	8.057	8.283	1.454
2446783.391	0.8079	8.010	8.094	8.335	1.474
2446829.294	0.7950	8.042	8.127	8.383	1.517
2447023.659	0.5339	8.048	8.142	8.509	2.006
2447072.590	0.4331	7.951	8.053	8.425	1.987
2447077.644	0.6247	8.109	8.194	8.571	1.989
2447148.376	0.2910	7.911	8.007	8.333	1.853
2447431.631	0.1627	7.904	8.010	8.287	1.721
2447211.649	0.2470	7.891	7.996	8.346	1.843
2447212.640	0.8728	7.954	8.043	8.267	1.440
2447212.644	0.8754	7.948	8.034	8.273	1.447
2447212.661	0.8861	7.950	8.027	8.271	1.446
2447212.664	0.8880	7.946	8.034	8.273	1.450
2447212.706	0.9145	7.925	8.015	8.257	1.461
2447212.709	0.9164	7.919	8.015	8.253	1.466
2447219.617	0.2787	7.882	7.988	8.344	1.871
2447219.621	0.2812	7.884	7.990	8.333	1.871
2447219.678	0.3172	7.914	8.003	8.329	1.876
2447219.710	0.3374	7.903	8.007	8.349	1.910
2447220.655	0.9342	7.912	8.009	8.247	1.460
2447460.892	0.6406	8.125	8.228	8.570	1.962
2447460.974	0.6924	8.146	8.252	8.583	1.915
2447461.017	0.7196	8.171	8.274	8.601	1.855
2447462.792	0.8405	7.986	8.052	8.297	1.407
2447462.990	0.9655	7.902	7.986	8.221	1.450
2447465.796	0.7374	8.157	8.249	8.571	1.805
2447465.846	0.7690	8.101	8.193	8.485	1.652
2447465.921	0.8164	8.021	8.094	8.325	1.425
2447465.983	0.8555	7.955	8.044	8.281	1.434
2447466.023	0.8808	7.960	8.049	8.275	1.436
2447466.764	0.3487	7.922	8.019	8.356	1.904
2447466.828	0.3891	7.921	8.039	8.378	1.955
2447466.868	0.4144	7.947	8.050	8.401	1.964
2447466.906	0.4384	7.965	8.059	8.425	1.981
2447466.944	0.4624	7.987	8.073	8.434	1.994
2447466.985	0.4883	7.997	8.093	8.457	2.018
2447467.026	0.5142	8.028	8.134	8.486	2.011
2447468.838	0.6584	8.123	8.224	8.580	1.952
2447468.995	0.7576	8.110	8.208	8.531	1.729
2447469.019	0.7727	8.096	8.179	8.479	1.629

APPENDIX B: THE DERIVATION OF MEAN JHK_s MAGNITUDES FOR RR LYRAE STARS WITH 2MASS MAGNITUDES.

The 2MASS Catalogue (Cutri et al. 2003) gives JHK_s magnitudes for a single Julian Date. The derivation of the mean magnitudes (hereafter $\langle J \rangle, \langle H \rangle, \langle K_s \rangle$) requires (a) ephemerides for each star that will give a phase for the 2MASS data that is accurate to at least 0.1, (b) a visual amplitude (ΔV) for the RR Lyrae star and (c) a standard light curve (or template) in each of J, H & K_s which may be converted to the J, H and K_s light curves of the star in question by means of its ΔV . Jones, Carney & Fullbright (1996) gave templates of $K - \langle K \rangle$ vs phase for a number of ranges of their B -amplitude for type ab RR Lyrae stars; a single template was given for type c variables. The method that we describe below covers J, H and K_s and gives tables (rather than plots) from which the mean magnitudes can be computed.

B1.1 Ephemerides and visual amplitudes.

The 2MASS observations were made in the period 1997 to 2000. We therefore need to get a time of maximum light (JD(max)) for each variable that is as near to this epoch as possible. Fortunately a JD(max) for most of our variables can be found either in the ASAS catalogue (Pojmanski, 2002) which covers the sky south of declination $+28^\circ$ with epochs since 1997 or in the compilation by Wils et al. (2006) for epochs 1999 to 2000 for stars north of declination -38° . In other cases, recent JD(max) are cited by Maintz (2005). Periods were primarily taken from the ASAS catalogue (loc. cit.) or Maintz (loc. cit.). The majority of the ΔV s were taken from the catalogue of Nikolov, Buchantsova & Frolov (1984), the ASAS catalogue (loc. cit.) or Schmidt (1991). In some cases, the Hipparcos amplitude was multiplied by 0.874 to get ΔV . This data allowed us to derive both the phase of the 2MASS data and ΔV for each variable.

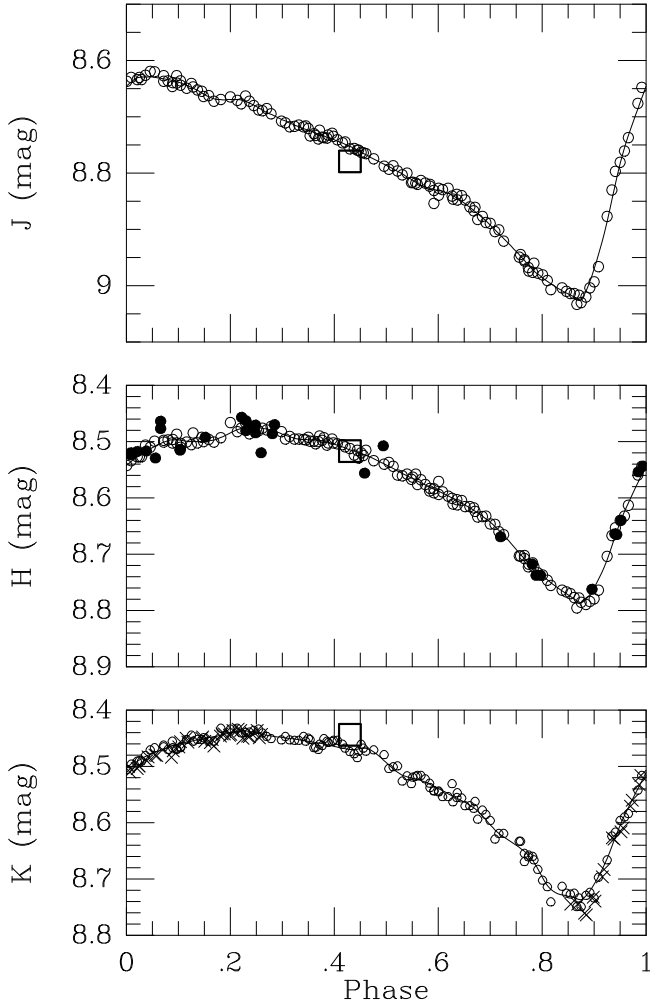


Figure B1. The JHK light curves of SW And. The open circles are from observations of Barnes et al. (1992), the crosses from those of Jones et al. (1992) and the filled circles are Kinman’s unpublished observations. The 2MASS observations are shown as the large open squares.

B1.2 A standard RR Lyrae light curve for J, H & K_s

Jones, Carney & Fulbright (1996) noted that the RRab K light curves showed small differences in their shapes that were a function of amplitude. They therefore provided templates of $K - \langle K \rangle$ as a function of phase (ϕ) for stars in five different ranges of B -amplitude. These templates were derived from the K light curves of field RR Lyrae stars that had been observed by several authors. We chose to produce a template of a single well observed RR Lyrae star (SW And) of intermediate amplitude. Excellent light curves in J, H & K have been given for SW And by Barnes et al. (1992). These were based on observations made in 1988; they also gave $BVRI$ data for the same year. Jones et al. (1992) gave a partial KBV light curve for SW And based on observations made in 1987. In addition 31 unpublished observations in H made by Kinman between November 1987 and November 1989 were also available. All these infrared observations were made using the Kitt Peak 1.3-m telescope and are shown in Fig. B1 using the ephemeris:

$$JD(max) = 24443067.6819 + 0.44226582 \times E \quad (9)$$

The agreement between the three data sets shows that the light curve is stable. The 2MASS observations were made twelve years later ($JD = 24450739.8477$) and the phase (0.426) was determined from an ephemeris derived from the period given by Maintz (2005) and the JD (max) given by Wils et al. (2006):

$$JD(max) = 24451416.3203 + 0.442262 \times E \quad (10)$$

The 2MASS observations (open squares) show good agreement with the light curves given in Fig. B1. The intensity-weighted $\langle J \rangle$, $\langle H \rangle$ & $\langle K \rangle$ of SW And are 8.780, 8.575 & 8.575 respectively. The corrections to be applied to the J, H & K magnitudes of this star as a function of phase to get the intensity-weighted mean magnitudes are given in Table B1. These corrections must be multiplied by a factor which takes into account the difference between the amplitude ΔV of SW And and that of the variable under consideration.

B1.3 The correction for the amplitude of the variable

A literature search for RR*ab* Lyrae stars with reliable infrared light-curves gave 11, 13 & 27 with *J*, *H* & *K* amplitudes respectively. These infrared amplitudes are shown plotted against their corresponding *V* amplitudes in Fig. B2 with the following linear fits:

$$\Delta J = -0.015 + 0.450 \times \Delta V \tag{11}$$

$$\Delta H = 0.111 + 0.206 \times \Delta V \tag{12}$$

$$\Delta K = 0.176 + 0.125 \times \Delta V \tag{13}$$

Table B1: Corrections to JHK as function of phase.

Phase	J	ΔJ	H	ΔH	K	ΔK
0.0000	8.6450	0.1350	8.5420	0.0330	8.5110	0.0210
0.0050	8.6415	0.1385	8.5383	0.0367	8.5061	0.0259
0.0100	8.6376	0.1424	8.5345	0.0405	8.5010	0.0310
0.0150	8.6339	0.1461	8.5308	0.0442	8.4960	0.0360
0.0200	8.6311	0.1489	8.5274	0.0476	8.4917	0.0403
0.0250	8.6299	0.1501	8.5245	0.0505	8.4884	0.0436
0.0300	8.6294	0.1506	8.5217	0.0533	8.4858	0.0462
0.0350	8.6291	0.1509	8.5189	0.0561	8.4834	0.0486
0.0400	8.6291	0.1509	8.5161	0.0589	8.4811	0.0509
0.0450	8.6292	0.1508	8.5134	0.0616	8.4789	0.0531
0.0500	8.6296	0.1504	8.5107	0.0643	8.4769	0.0551
0.0550	8.6300	0.1500	8.5081	0.0669	8.4750	0.0570
0.0600	8.6306	0.1494	8.5057	0.0693	8.4731	0.0589
0.0650	8.6313	0.1487	8.5035	0.0715	8.4714	0.0606
0.0700	8.6321	0.1479	8.5015	0.0735	8.4697	0.0623
0.0750	8.6330	0.1470	8.4997	0.0753	8.4680	0.0640
0.0800	8.6338	0.1462	8.4983	0.0767	8.4663	0.0657
0.0850	8.6348	0.1452	8.4972	0.0778	8.4647	0.0673
0.0900	8.6359	0.1441	8.4968	0.0782	8.4632	0.0688
0.0950	8.6372	0.1428	8.4969	0.0781	8.4619	0.0701
0.1000	8.6387	0.1413	8.4973	0.0777	8.4607	0.0713
0.1050	8.6403	0.1397	8.4979	0.0771	8.4595	0.0725
0.1100	8.6420	0.1380	8.4986	0.0764	8.4584	0.0736
0.1150	8.6438	0.1362	8.4993	0.0757	8.4573	0.0747
0.1200	8.6457	0.1343	8.4998	0.0752	8.4563	0.0757
0.1250	8.6476	0.1324	8.5000	0.0750	8.4552	0.0768
0.1300	8.6497	0.1303	8.5000	0.0750	8.4542	0.0778
0.1350	8.6521	0.1279	8.5000	0.0750	8.4532	0.0788
0.1400	8.6547	0.1253	8.4999	0.0751	8.4522	0.0798
0.1450	8.6575	0.1225	8.4998	0.0752	8.4513	0.0807
0.1500	8.6602	0.1198	8.4996	0.0754	8.4504	0.0816
0.1550	8.6627	0.1173	8.4993	0.0757	8.4495	0.0825
0.1600	8.6650	0.1150	8.4987	0.0763	8.4486	0.0834
0.1650	8.6669	0.1131	8.4979	0.0771	8.4477	0.0843
0.1700	8.6682	0.1118	8.4967	0.0783	8.4468	0.0852
0.1750	8.6691	0.1109	8.4952	0.0798	8.4458	0.0862
0.1800	8.6695	0.1105	8.4934	0.0816	8.4447	0.0873
0.1850	8.6697	0.1103	8.4913	0.0837	8.4435	0.0885
0.1900	8.6697	0.1103	8.4891	0.0859	8.4424	0.0896
0.1950	8.6695	0.1105	8.4868	0.0882	8.4412	0.0908
0.2000	8.6693	0.1107	8.4845	0.0905	8.4401	0.0919
0.2050	8.6692	0.1108	8.4822	0.0928	8.4391	0.0929
0.2100	8.6693	0.1107	8.4802	0.0948	8.4383	0.0937
0.2150	8.6695	0.1105	8.4784	0.0966	8.4376	0.0944
0.2200	8.6702	0.1098	8.4769	0.0981	8.4372	0.0948
0.2250	8.6713	0.1087	8.4758	0.0992	8.4370	0.0950
0.2300	8.6728	0.1072	8.4751	0.0999	8.4372	0.0948
0.2350	8.6747	0.1053	8.4747	0.1003	8.4377	0.0943
0.2400	8.6769	0.1031	8.4746	0.1004	8.4384	0.0936
0.2450	8.6793	0.1007	8.4746	0.1004	8.4394	0.0926
0.2500	8.6819	0.0981	8.4749	0.1001	8.4405	0.0915
0.2550	8.6845	0.0955	8.4754	0.0996	8.4416	0.0904
0.2600	8.6872	0.0928	8.4760	0.0990	8.4427	0.0893
0.2650	8.6897	0.0903	8.4768	0.0982	8.4438	0.0882
0.2700	8.6921	0.0879	8.4776	0.0974	8.4447	0.0873
0.2750	8.6943	0.0857	8.4786	0.0964	8.4454	0.0866
0.2800	8.6965	0.0835	8.4799	0.0951	8.4461	0.0859
0.2850	8.6987	0.0813	8.4813	0.0937	8.4468	0.0852
0.2900	8.7008	0.0792	8.4830	0.0920	8.4474	0.0846
0.2950	8.7030	0.0770	8.4848	0.0902	8.4480	0.0840
0.3000	8.7051	0.0749	8.4866	0.0884	8.4486	0.0834
0.3050	8.7072	0.0728	8.4884	0.0866	8.4492	0.0828
0.3100	8.7092	0.0708	8.4902	0.0848	8.4498	0.0822
0.3150	8.7113	0.0687	8.4919	0.0831	8.4504	0.0816

Continued on Next Page...

Phase	J	ΔJ	H	ΔH	K	ΔK
0.3200	8.7133	0.0667	8.4933	0.0817	8.4511	0.0809
0.3250	8.7152	0.0648	8.4946	0.0804	8.4517	0.0803
0.3300	8.7171	0.0629	8.4955	0.0795	8.4524	0.0796
0.3350	8.7189	0.0611	8.4961	0.0789	8.4531	0.0789
0.3400	8.7207	0.0593	8.4964	0.0786	8.4538	0.0782
0.3450	8.7224	0.0576	8.4965	0.0785	8.4545	0.0775
0.3500	8.7240	0.0560	8.4966	0.0784	8.4552	0.0768
0.3550	8.7256	0.0544	8.4966	0.0784	8.4559	0.0761
0.3600	8.7273	0.0527	8.4966	0.0784	8.4567	0.0753
0.3650	8.7289	0.0511	8.4969	0.0781	8.4575	0.0745
0.3700	8.7306	0.0494	8.4974	0.0776	8.4583	0.0737
0.3750	8.7324	0.0476	8.4982	0.0768	8.4592	0.0728
0.3800	8.7341	0.0459	8.4992	0.0758	8.4601	0.0719
0.3850	8.7358	0.0442	8.5004	0.0746	8.4612	0.0708
0.3900	8.7376	0.0424	8.5018	0.0732	8.4623	0.0697
0.3950	8.7393	0.0407	8.5032	0.0718	8.4634	0.0686
0.4000	8.7410	0.0390	8.5047	0.0703	8.4646	0.0674
0.4050	8.7428	0.0372	8.5063	0.0687	8.4657	0.0663
0.4100	8.7446	0.0354	8.5079	0.0671	8.4668	0.0652
0.4150	8.7465	0.0335	8.5095	0.0655	8.4678	0.0642
0.4200	8.7484	0.0316	8.5111	0.0639	8.4687	0.0633
0.4250	8.7504	0.0296	8.5127	0.0623	8.4695	0.0625
0.4300	8.7524	0.0276	8.5143	0.0607	8.4701	0.0619
0.4350	8.7546	0.0254	8.5158	0.0592	8.4702	0.0618
0.4400	8.7570	0.0230	8.5173	0.0577	8.4697	0.0623
0.4450	8.7594	0.0206	8.5189	0.0561	8.4689	0.0631
0.4500	8.7619	0.0181	8.5205	0.0545	8.4682	0.0638
0.4550	8.7645	0.0155	8.5221	0.0529	8.4678	0.0642
0.4600	8.7670	0.0130	8.5239	0.0511	8.4679	0.0641
0.4650	8.7695	0.0105	8.5258	0.0492	8.4689	0.0631
0.4700	8.7720	0.0080	8.5278	0.0472	8.4709	0.0611
0.4750	8.7744	0.0056	8.5300	0.0450	8.4737	0.0583
0.4800	8.7768	0.0032	8.5322	0.0428	8.4770	0.0550
0.4850	8.7791	0.0009	8.5345	0.0405	8.4808	0.0512
0.4900	8.7815	-0.0015	8.5368	0.0382	8.4848	0.0472
0.4950	8.7839	-0.0039	8.5392	0.0358	8.4891	0.0429
0.5000	8.7863	-0.0063	8.5415	0.0335	8.4934	0.0386
0.5050	8.7887	-0.0087	8.5440	0.0310	8.4977	0.0343
0.5100	8.7911	-0.0111	8.5464	0.0286	8.5019	0.0301
0.5150	8.7935	-0.0135	8.5488	0.0262	8.5058	0.0262
0.5200	8.7960	-0.0160	8.5512	0.0238	8.5093	0.0227
0.5250	8.7985	-0.0185	8.5535	0.0215	8.5124	0.0196
0.5300	8.8011	-0.0211	8.5559	0.0191	8.5150	0.0170
0.5350	8.8038	-0.0238	8.5582	0.0168	8.5170	0.0150
0.5400	8.8067	-0.0267	8.5606	0.0144	8.5186	0.0134
0.5450	8.8095	-0.0295	8.5629	0.0121	8.5199	0.0121
0.5500	8.8124	-0.0324	8.5653	0.0097	8.5210	0.0110
0.5550	8.8152	-0.0352	8.5676	0.0074	8.5221	0.0099
0.5600	8.8179	-0.0379	8.5700	0.0050	8.5232	0.0088
0.5650	8.8205	-0.0405	8.5723	0.0027	8.5244	0.0076
0.5700	8.8228	-0.0428	8.5746	0.0004	8.5259	0.0061
0.5750	8.8248	-0.0448	8.5769	-0.0019	8.5278	0.0042
0.5800	8.8264	-0.0464	8.5792	-0.0042	8.5298	0.0022
0.5850	8.8277	-0.0477	8.5814	-0.0064	8.5320	0.0000
0.5900	8.8287	-0.0487	8.5836	-0.0086	8.5343	-0.0023
0.5950	8.8297	-0.0497	8.5857	-0.0107	8.5366	-0.0046
0.6000	8.8306	-0.0506	8.5879	-0.0129	8.5390	-0.0070
0.6050	8.8316	-0.0516	8.5901	-0.0151	8.5415	-0.0095
0.6100	8.8328	-0.0528	8.5924	-0.0174	8.5440	-0.0120
0.6150	8.8343	-0.0543	8.5947	-0.0197	8.5465	-0.0145
0.6200	8.8361	-0.0561	8.5970	-0.0220	8.5490	-0.0170
0.6250	8.8384	-0.0584	8.5995	-0.0245	8.5515	-0.0195
0.6300	8.8410	-0.0610	8.6019	-0.0269	8.5538	-0.0218
0.6350	8.8438	-0.0638	8.6043	-0.0293	8.5561	-0.0241
0.6400	8.8468	-0.0668	8.6067	-0.0317	8.5583	-0.0263
0.6450	8.8499	-0.0699	8.6092	-0.0342	8.5606	-0.0286

Continued on Next Page...

Phase	J	ΔJ	H	ΔH	K	ΔK
0.6500	8.8533	-0.0733	8.6117	-0.0367	8.5630	-0.0310
0.6550	8.8567	-0.0767	8.6143	-0.0393	8.5655	-0.0335
0.6600	8.8602	-0.0802	8.6170	-0.0420	8.5683	-0.0363
0.6650	8.8639	-0.0839	8.6198	-0.0448	8.5713	-0.0393
0.6700	8.8675	-0.0875	8.6228	-0.0478	8.5746	-0.0426
0.6750	8.8712	-0.0912	8.6259	-0.0509	8.5783	-0.0463
0.6800	8.8752	-0.0952	8.6291	-0.0541	8.5827	-0.0507
0.6850	8.8792	-0.0992	8.6324	-0.0574	8.5877	-0.0557
0.6900	8.8834	-0.1034	8.6358	-0.0608	8.5929	-0.0609
0.6950	8.8878	-0.1078	8.6394	-0.0644	8.5983	-0.0663
0.7000	8.8922	-0.1122	8.6432	-0.0682	8.6037	-0.0717
0.7050	8.8967	-0.1167	8.6472	-0.0722	8.6088	-0.0768
0.7100	8.9013	-0.1213	8.6514	-0.0764	8.6135	-0.0815
0.7150	8.9058	-0.1258	8.6558	-0.0808	8.6176	-0.0856
0.7200	8.9104	-0.1304	8.6605	-0.0855	8.6213	-0.0893
0.7250	8.9151	-0.1351	8.6654	-0.0904	8.6247	-0.0927
0.7300	8.9199	-0.1399	8.6705	-0.0955	8.6279	-0.0959
0.7350	8.9246	-0.1446	8.6757	-0.1007	8.6309	-0.0989
0.7400	8.9295	-0.1495	8.6810	-0.1060	8.6339	-0.1019
0.7450	8.9343	-0.1543	8.6863	-0.1113	8.6369	-0.1049
0.7500	8.9392	-0.1592	8.6916	-0.1166	8.6399	-0.1079
0.7550	8.9441	-0.1641	8.6969	-0.1219	8.6431	-0.1111
0.7600	8.9490	-0.1690	8.7020	-0.1270	8.6466	-0.1146
0.7650	8.9541	-0.1741	8.7070	-0.1320	8.6503	-0.1183
0.7700	8.9597	-0.1797	8.7119	-0.1369	8.6543	-0.1223
0.7750	8.9652	-0.1852	8.7167	-0.1417	8.6591	-0.1271
0.7800	8.9701	-0.1901	8.7211	-0.1461	8.6647	-0.1327
0.7850	8.9743	-0.1943	8.7254	-0.1504	8.6716	-0.1396
0.7900	8.9782	-0.1982	8.7296	-0.1546	8.6795	-0.1475
0.7950	8.9819	-0.2019	8.7337	-0.1587	8.6880	-0.1560
0.8000	8.9855	-0.2055	8.7378	-0.1628	8.6964	-0.1644
0.8050	8.9890	-0.2090	8.7418	-0.1668	8.7045	-0.1725
0.8100	8.9922	-0.2122	8.7456	-0.1706	8.7115	-0.1795
0.8150	8.9954	-0.2154	8.7493	-0.1743	8.7171	-0.1851
0.8200	8.9984	-0.2184	8.7528	-0.1778	8.7211	-0.1891
0.8250	9.0015	-0.2215	8.7564	-0.1814	8.7240	-0.1920
0.8300	9.0044	-0.2244	8.7598	-0.1848	8.7262	-0.1942
0.8350	9.0073	-0.2273	8.7631	-0.1881	8.7277	-0.1957
0.8400	9.0100	-0.2300	8.7664	-0.1914	8.7288	-0.1968
0.8450	9.0125	-0.2325	8.7695	-0.1945	8.7296	-0.1976
0.8500	9.0149	-0.2349	8.7725	-0.1975	8.7304	-0.1984
0.8550	9.0169	-0.2369	8.7754	-0.2004	8.7313	-0.1993
0.8600	9.0189	-0.2389	8.7782	-0.2032	8.7326	-0.2006
0.8650	9.0217	-0.2417	8.7817	-0.2067	8.7346	-0.2026
0.8700	9.0240	-0.2440	8.7848	-0.2098	8.7364	-0.2044
0.8750	9.0235	-0.2435	8.7860	-0.2110	8.7366	-0.2046
0.8800	9.0180	-0.2380	8.7840	-0.2090	8.7340	-0.2020
0.8850	9.0084	-0.2284	8.7793	-0.2043	8.7291	-0.1971
0.8900	8.9971	-0.2171	8.7735	-0.1985	8.7233	-0.1913
0.8950	8.9843	-0.2043	8.7668	-0.1918	8.7166	-0.1846
0.9000	8.9702	-0.1902	8.7592	-0.1842	8.7093	-0.1773
0.9050	8.9551	-0.1751	8.7508	-0.1758	8.7013	-0.1693
0.9100	8.9392	-0.1592	8.7417	-0.1667	8.6927	-0.1607
0.9150	8.9227	-0.1427	8.7320	-0.1570	8.6837	-0.1517
0.9200	8.9055	-0.1255	8.7216	-0.1466	8.6742	-0.1422
0.9250	8.8862	-0.1062	8.7098	-0.1348	8.6635	-0.1315
0.9300	8.8656	-0.0856	8.6969	-0.1219	8.6520	-0.1200
0.9350	8.8442	-0.0642	8.6834	-0.1084	8.6400	-0.1080
0.9400	8.8228	-0.0428	8.6696	-0.0946	8.6279	-0.0959
0.9450	8.8021	-0.0221	8.6562	-0.0812	8.6159	-0.0839
0.9500	8.7829	-0.0029	8.6434	-0.0684	8.6045	-0.0725
0.9550	8.7658	0.0142	8.6318	-0.0568	8.5940	-0.0620
0.9600	8.7502	0.0298	8.6209	-0.0459	8.5841	-0.0521
0.9650	8.7357	0.0443	8.6105	-0.0355	8.5745	-0.0425
0.9700	8.7220	0.0580	8.6004	-0.0254	8.5652	-0.0332
0.9750	8.7089	0.0711	8.5905	-0.0155	8.5560	-0.0240

Continued on Next Page...

Phase	J	ΔJ	H	ΔH	K	ΔK
0.9800	8.6961	0.0839	8.5808	-0.0058	8.5470	-0.0150
0.9850	8.6836	0.0964	8.5712	0.0038	8.5381	-0.0061
0.9900	8.6710	0.1090	8.5616	0.0134	8.5292	0.0028
0.9950	8.6582	0.1218	8.5519	0.0231	8.5201	0.0119
1.0000	8.6450	0.1350	8.5420	0.0330	8.5110	0.0210

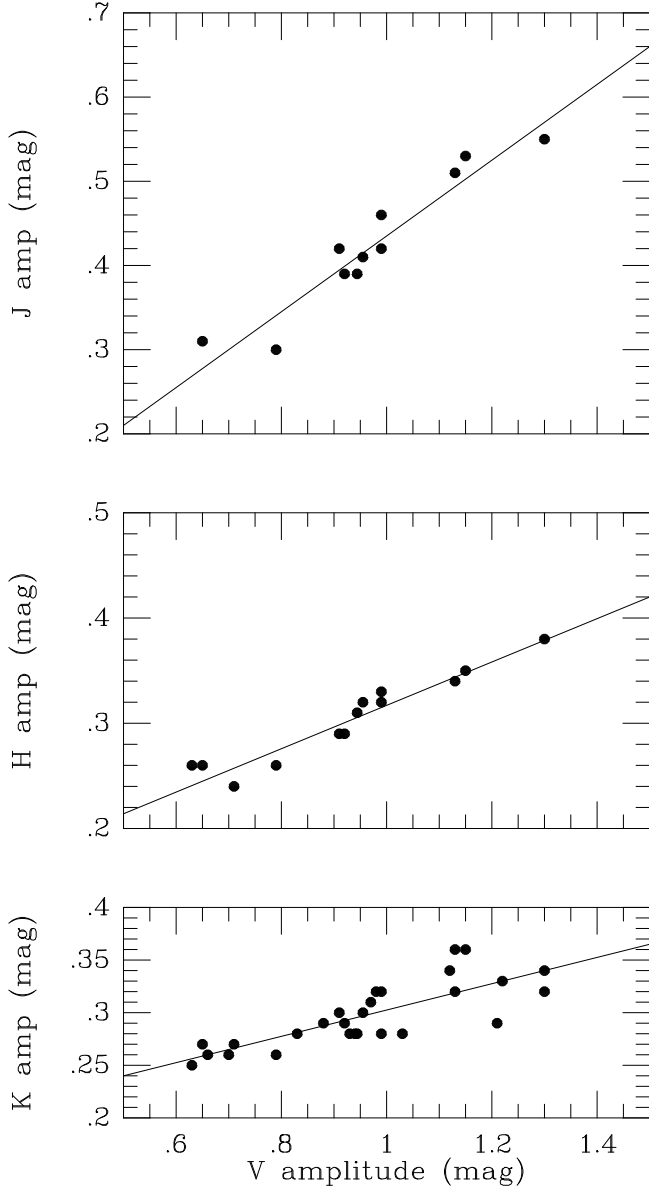


Figure B2. The relation between the J , H and K amplitudes and their V amplitudes for RR Lyrae stars that have well determined light curves.

The J , H & K amplitudes of SW And are 0.395, 0.314 & 0.300 respectively. The corrections in Table B1 must therefore be multiplied by the following factors for a type ab variable with amplitude ΔV :

$$-0.038 + 1.139 \times \Delta V \quad \text{for } J; \quad (14)$$

$$0.358 + 0.665 \times \Delta V \quad \text{for } H; \quad (15)$$

$$0.594 + 0.417 \times \Delta V \quad \text{for } K. \quad (16)$$

These corrections must be added to the observed magnitudes to obtain the mean magnitudes. In the case of RRc variables (which have quite low amplitudes) the above corrections can also be applied for the J magnitudes, while the $K - \langle K \rangle$ correction of Jones et al. (*loc. cit.*) can be applied to both the H and K magnitudes to get the mean magnitudes.

B1.4 The accuracy of these corrections

Table B2 compares the mean magnitudes $\langle J \rangle$, $\langle H \rangle$ & $\langle K_s \rangle$ derived from 2MASS data (Source 1) with those derived from the data of Fernley et al. (1993) (Source 2) and from unpublished H magnitudes of Kinman (Source 3). The largest discrepancies are for RZ Cep which is multiperiodic and has a double-peaked maximum (Cester & Todoran 1976). The second observation of RR Lyrae by Fernley et al. (1993) (indicated by an asterisk in Table B2) was taken near maximum light. RR Lyrae shows a Blazhko effect of varying period so the large discrepancy between this and the other two observations is not surprising. If we neglect these observations, the mean differences in the sense (Fernley et al. *minus* 2MASS) are $+0.006 \pm 0.013$, $+0.008 \pm 0.015$ & $+0.008 \pm 0.0015$ mag for $\langle J \rangle$, $\langle H \rangle$ & $\langle K_s \rangle$ respectively. The mean difference (Kinman *minus* 2MASS) is -0.006 ± 0.006 for $\langle H \rangle$. These differences do not disagree with the small differences expected between observations made using the standards of Elias et al. (1982, 1983) as was the case of the Fernley et al. and the Kinman data and those on the 2MASS system (Carpenter 2001). It must be remembered that errors of as much as 0.2 mag can occur near the rising branch or with stars with varying light-curves and/or ephemerides.

Table B2. comparison of 2MASS mean magnitudes with those derived from other sources.

Star	$\langle J \rangle$	$\langle H \rangle$	$\langle K_s \rangle$	Source
(1)	(2)	(3)	(4)	(5)
SW AND	8.807	8.578	8.506	(1)
	...	8.573	...	(3)
TU UMA	8.907	8.728	8.654	(1)
	...	8.714	...	(3)
BH PEG	9.345	9.085	9.041	(1)
	9.345	9.065	9.025	(2)
	9.395	9.055	9.009	(2)
	...	9.106	...	(3)
RR LYR	6.739	6.511	6.462	(1)
	6.780	6.530	6.490	(2)
	6.930	6.670	6.650	(2)*
SV ERI	8.947	8.703	8.636	(1)
	8.915	8.672	8.658	(2)
	8.934	8.700	8.615	(2)
	...	8.682	...	(3)
RZ CEP	8.251	8.068	7.998	(1)
	8.350	8.270	8.160	(2)
	8.360	8.140	8.140	(2)
XZ CYG	8.914	8.751	8.682	(1)
	8.970	8.790	8.770	(2)
	8.890	8.820	8.680	(2)
	...	8.730	...	(3)
DX DEL	9.001	8.741	8.682	(1)
	...	8.736	...	(3)
X ARI	8.327	8.026	7.928	(1)
	...	8.030	...	(3)